SMC-BMC DİZAYN KRİTERLERİ

SMC-BMC DESIGN CRİTERİONS

Metin BAŞBUDAK

Tongün A.Ş. , TÜRKİYE

metinbasbudak@superonline.com

Abstract

The European market for fibre reinforced plastics has an annual volume of more than 1.3 million tons. SMC-BMC represent the biggest segment within the group o materials.
Both products provide a wide range of physical properties and appearence characteristics enabling their use in passenger cars, trucks, public transport , electrical and construcktion.

SMC-BMC Composition

They consist of a thermosetting resin, glass fibre reinforcement and filler. Additional ingredients are low profile components, cure initiators, thickeners, process additives and mold releasing agents.
SMC-BMC can be formulated to meet specific performance requirements of particular application such as tensile loading or class A surface.
Allthough SMC and BMC have the same ingredients their manufacturing processes and physical characteristics are different.
SMC and BMC manufacturing processes are shown in figures and physical properties in comparison tables.
SMC and BMC can be molded in similar tools under heat and presure. There are three possibilities for molding SMC-BMC:

- Compresion Molding
- Transfer Molding
- Enjection Molding

Recommended Design Using SMC-BMC

SMC-BMC offers many advantages in part consolidation, corrosion resistance, reduced mass and lowe capital investment on lower production runs.

- Review the Design Theme –cooperation with designer and moulder is very important
- Preliminary Structural Evalution-after completing CAD model of the part loadings can be evaluated using finite element analysis (FEA)
- Basic Design Details
  - Minimum Contour
  - Part Thickness-nominal part thickness is recommended 2.0-3.0 mm for outerpanels and 1.75-2.5 mm for iner panels
  - Radii-radii are determined by painting and moulding considarations
  - Moldability-inside corner radii 2.0 mm outercorner 1.5 mm
  - Radii guidlines for paintability-inner and outer radii as large as possible
  - Mash offs-a mash off is a localised reduction in panel thickness to create a membran.

Designing to Maximise Structure

One Piece Panel:

- Ribs-with ribs and bosses advantage over steel
- Place ribs opposite styling lines- the sink will be hidden through changing surface
- Rib geometry-the base of ribs should be 75 % of nominal panel thickness. For non appearance surface the base of the rib can be equal of the nominal thickness.
- Boss geometry-figure shows recommended drafts and radii
  - Boss geometry to maximize fastener performances-figure shows recommendations to maximize the fastener performances
  - Edge Design Details for Stiffness-using of flanges instead of thickening increases the stiffness of the part.

Two Piece Panel:

Two piece panel consist of inner and outer panels bonded together.

Panel Design and Construction

Design to Control Critical Dimensions

- Tolerancing-SMC-BMC has tolerances that affect dimentional reproducability
- Pres-press parallelism vary among pres manufacturers
- Mold-tooling tolerances can be +/- 0.25 mm for critical areas
- Material- material shrinkage tolerances must be considered
- Molded Datum Features-will increas repeatability in bonded assemblies

Özet

Avrupa elyaf takviyeli plastik pazarı yılda 1,5 milyon ton seviyesini geçmiş durumdadır. Bu pazarda en büyük payı SMC-BMC tüketimi almaktadır.

Bu iki ürün fiziksel özellikleri ve görüntü zenginliği nedeniyle otomobil,traktör, ticari araçlar,elektrik ve inşaat gibi bir çok sektörde geniş kullanım bulmuşlardır.

SMC-BMC Yapısı

Yapının ana komponentlerini termoset reçine, camelyaf takviye malzemesi ve dolgu malzemesi teşkil eder. Bunlardan başka low profile katkısı, sertleştirme inisiyatörleri, kıvamlaştırıcılar, proses katkıları ve kalıp ayırıcıları ilave edilmiştir.
Yapıdaki değişik komponentler yardımıyla isteğe uygun formül geliştirilmesi mümkün olmaktadır. Bu sayede kullanılma yerinin ihtiyaçlarına uygun olarak yüksek mekanik zorlamalara dirençli ve class A şartlarına uygun yüzeyli ürünler elde edilebilmektedir.
SMC ve BMC içerdiği komponentler açısında ve kullanım şekliyle aynı olmasına karşın üretim şekillerinde farklılık göstermektedirler. Bu farklılığı fiziksel özelliklerinde de görmek mümkündür.
SMC ve BMC farklı üretilse de aynı şekilde kalıplanmaktadırlar. Isıtılan çelik kalıplarda yüksek basınç altında gerçekleşen bu proses de yaygın olarak üç şekil görülmektedir.

- Presleme
- Transfer presleme
- Enjeksiyon

SMC-BMC ile Dizayn Tavsiyeleri:

SMC-BMC parça dizaynı için birçok avantaj sağlamaktadır. Bunların içinde ünitelerin konsolidasyonu,dış etkilere dayanıklılık, ağırlık tasarrufu, izolasyon kolaylığı, üretim hızı ve düşük sayılarda yatırım tasarrufu sayılabilir.

- Dizayn ön çalışması –parça tasarımcısı ve üreticiyle birlikte çalışılmalıdır
- Ön tasarımın değerlendirilmesi-CAD model hazırlandıktan sonra FEA ile yükleme sonuçları değerlendirilir
- Temel Dizayn Öğeleri
  - Minimum Kontur
  - Parça Kalınlığı-dış kabuk için önerilen kalınlık 2.0-3.0 mm-iç kabuk için 1.75-2.5 mm dir
  - Radyuslar- Resimde gösterilmektedir-
  - Kalıplama tavsiyesi-iç radyus 2.0 mm dış radyus 1.5 mm
  - Boyama kriterleri- iç ve dış radyuslar olabildiğince büyük olmalıdır.
  - Perde- perdelemek boşluk olacak yerlerin üzerinde parça kalınlığını düşürülmesidir.

Azami Sağlamlık Tasarımı

- Federler- federler ve cıvata boşluklarıyla çeliğe karşı avantaj sağlanabilmektedir.
- Federlerin çizgiye oturtulması-böylece olası çökmeler saklanabilir
- Feder geometrisi-görünür yüzeylerde feder kalınlıkları parça kalınlığının azami % 75 i kadar olmalıdır. Görünmiyen yüzeylerde feder dibi parça kalınlığı kadar olabilir.

- Boss geometrisi- resimde önerilen derinlik ve radyus görülmektedir
- Sağlamlığı artırmak için –resimde sağlamlığı artırma tavsiyeleri yeralmaktadır
- Sertliği artırmak için kenar dizaynı-kenarları kalınlaştırmak yerine flanş şekli parçayı daha rijid yapabilmektedir

İki Parça Birleşimi

İki parçalı konstruksiyonlar bir iç ve bir dış kabuğun yapıştırılmasıyla oluşmaktadır. Resimler bu şekilde oluşan parçaları göstermektedir.

Kritik Ölçüler Kontrolü İçin Dizayn Önerileri

- Toleranslar-SMC-BMC için geçerli toleranslar ölçülerin tekrarlanabilirliğini etkilemektedir
- Presler- pres üreticileri arasında pres paralelliği tolarensında farklılıklar bulunmaktadır
- Kalıp-kalıp toleransları +/- 0.25 mm ye kadar çıkabilmektedir
- Malzeme-malzeme reaksiyon çekmelerinde toleransı da hesaba katmak gerek
- Baskı tarihleri- kalıpta tarih damgası yapıştırılar parçalar için çok önemlidir.

Giriş

Avrupa elyaf takviyeli plastik pazarı yılda 1.5 milyon ton seviyesini geçmiş durumdadır. Bu pazarda en büyük payı SMC-BMC tüketimi almaktadır. Bu iki ürün fiziksel özellikleri ve görüntü zenginliği nedeniyle otomobil, traktör, ticari araçlar, elektro ve inşaat gibi birçok sektörde geniş kullanım bulmuşlardır.

SMC-BMC YAPISI

Yapının ana komponentlerini termoset reçineler, camelyaf takviye malzemeleri ve dolgu malzemeleri teşkil eder. Bunlardan başka low profile katkısı,sertleştirme inisiyatörleri,kıvamlaştırıcılar, proses katkıları ve kalıp ayırıcılar ilave edilirler.

Yapıdaki değişik komponentler yardımıyla SMC-BMC de her isteğe uygun formül geliştirilmesi mümkün olmaktadır.Bu sayede kullanım yerinin ihtiyaçlarına uygun olarak yüksek mekanik zorlamalara dirençli ve class A şartlarına uygun yüzeyli ürünler elde edilebilmektedir.

SMC ve BMC içerdikleri komponentler açısından ve kalıplama şartlarına göre aynı olmalarına karşın üretim şekillerinde farklılık göstermektedirler. Bu farklılık fiziksel özelliklerine de yansımaktadır.

SMC –BMC KARŞILAŞTIRMALI ÖZELLİKLER TABLOSU

Özellik	UP 25	UP 50	UP 20/40	BMC	Birim
Kopma Direnci MPa	65-80	124-204	300-350	30-40	
E-Modul GPa	8,5	12-20	25-30	6-8	
Eğme Direnci MPa	155-200	250-380	650-750	60-80	
Darbe Direnci kJ/m2	60-90	120-200	300-500	20-40	
Yoğunluk g/cm3	1.7-2.0	1.85-2.0	1.9	1.7 -1.9	

Bu tablolardan da anlaşılabileceği gibi SMC BMC ye oranla daha güçlü ve dayanıklı bir yapı sergilemektedir. Camelyafın kırpıldıktan sonra sadece iki taraftan sıkıştırılmış ve BMC de olduğu gibi karıştırılmamış olması asıl nedendir. BMC de bulamaç bir yoğurucuda karıştırıldığından elyafların kırılarak güç kaybetmesi kaçınılmazdır. Bu nedenle daha yüksek mekanik değerlerin gerektiği otomotif gibi sektörlerde SMC kullanımı çok artmıştır. BMC ise daha yüksek dolgu kaldırması ve homojen renklendirilebilmesi nedeniyle daha çok elektro sektöründe yaygınlaşmıştır.

SMC-BMC NİN AVANTAJLARI

- Dizayn Zenginliği
- Hafifliği
- Mekanik değerleri
- Termik Özellikleri
- Elektriki İzolasyonu
- Korozyona Direnci
- Üretim Hızı
- Reaksiyon Çekme Kontrolü
- Renklendirilebilmesi
- Montaj Avantajları
- Ekonomikliği

SMC ve BMC üretimleri farklı olsa da kalıplanma şekilleri aynıdır. Isıtılan çelik kalıplarda yüksek basınç altında gerçekleşen bu proseste yaygın olarak üç şekil görülmektedir.

- Dikey Presleme
- Transfer Presleme
- Enjeksiyon Presleme

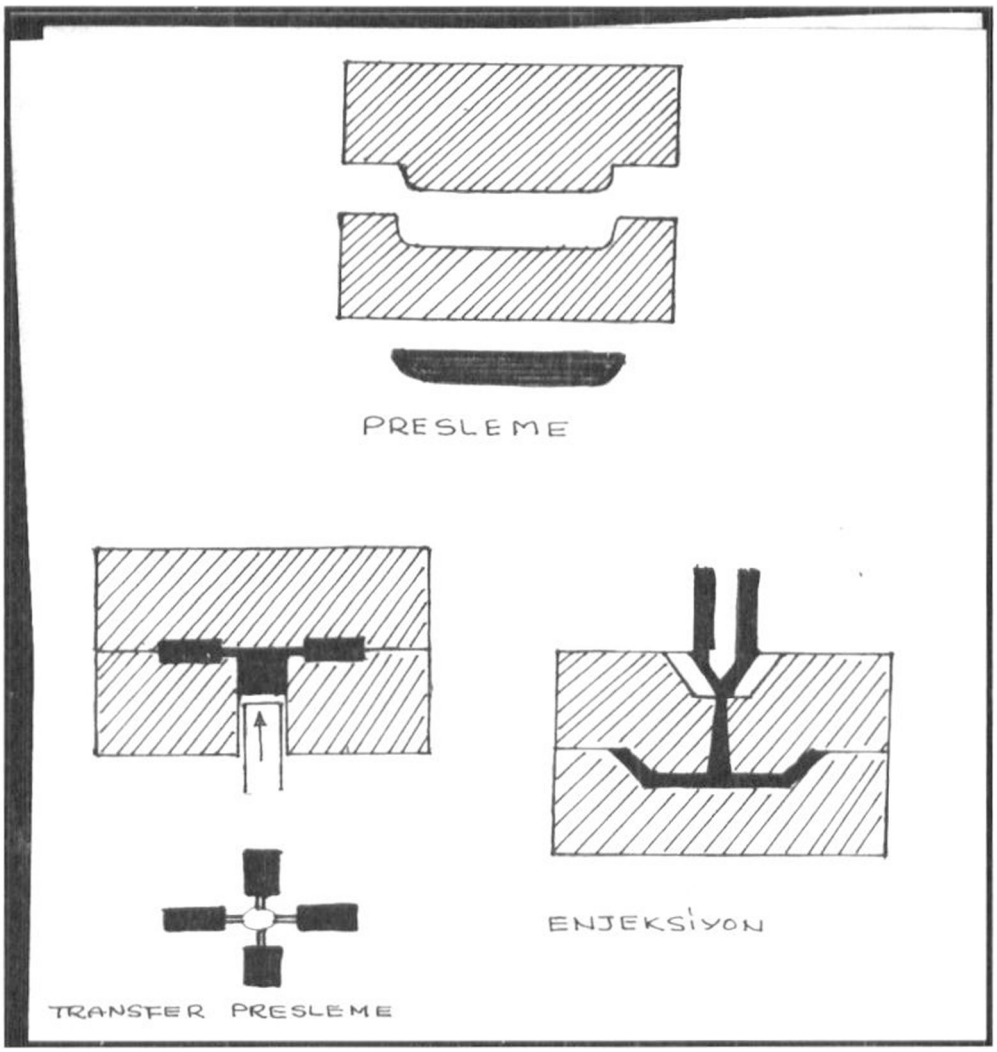
PRESLEME
ENJEKSİYON
TRANSFER PRESLEME

SMC-BMC ile Dizayn Tavsiyeleri

SMC-BMC parça dizaynı için birçok avantaj sağlamaktadır. Bunların içinde ünitelerin konsolidasyonu, dış etkilere dayanıklılık, ağırlık tasarrufu, izolasyon kolaylığı, üretim hızı düşük üretim miktarları için yatırım tasarrufu sayılabilir.

Dizayn edilecek parça için önemli veriler toplanarak SMC-BMC özellikleri ile karşılaştırılmalı ve klasik malzemelere üstünlüğü saptanmalıdır.

Dizayn çalışmalarında şu adımlar önemlidir:

- Dizayn ön çalışması – çalışmanın verimli olması için mutlaka parça tasarımcısı ve üreticiyle birlikte çalışılmalıdır
- Ön tasarımın değerlendirilmesi – parçanın hazırlanan CAD modeli beklenen yüklere dayanımı açısından FEA (finite elemantary analysis) ile kontrol edilmelidir
- Temel Dizayn Öğeleri – dizayn kriterleri açısından en önemli öğeler şunlardır
    - Minimum Kontur-düz yüzeyler imkan ölçüsünde küçük tutulmalıdır
    - Parça Kalınlığı – mümkünse kalınlık bütün parça boyunca eşit tutulmalıdır.Önerilen dış kabuk kalınlığı 2.0-3.0 mm, iç kabuk kalınlığı 1.75-2.5 mmdir
    - Radyuslar resimde gösteridiği gibi oldukca yumşak olmalıdır
    - Kalıplama Tavsiyesi- iç radyus 2 mm,dış radyus 1.5 mm
    - Boyama Kriterleri-iç ve dış radyuslar olabildiğince büyük tutulmalıdır

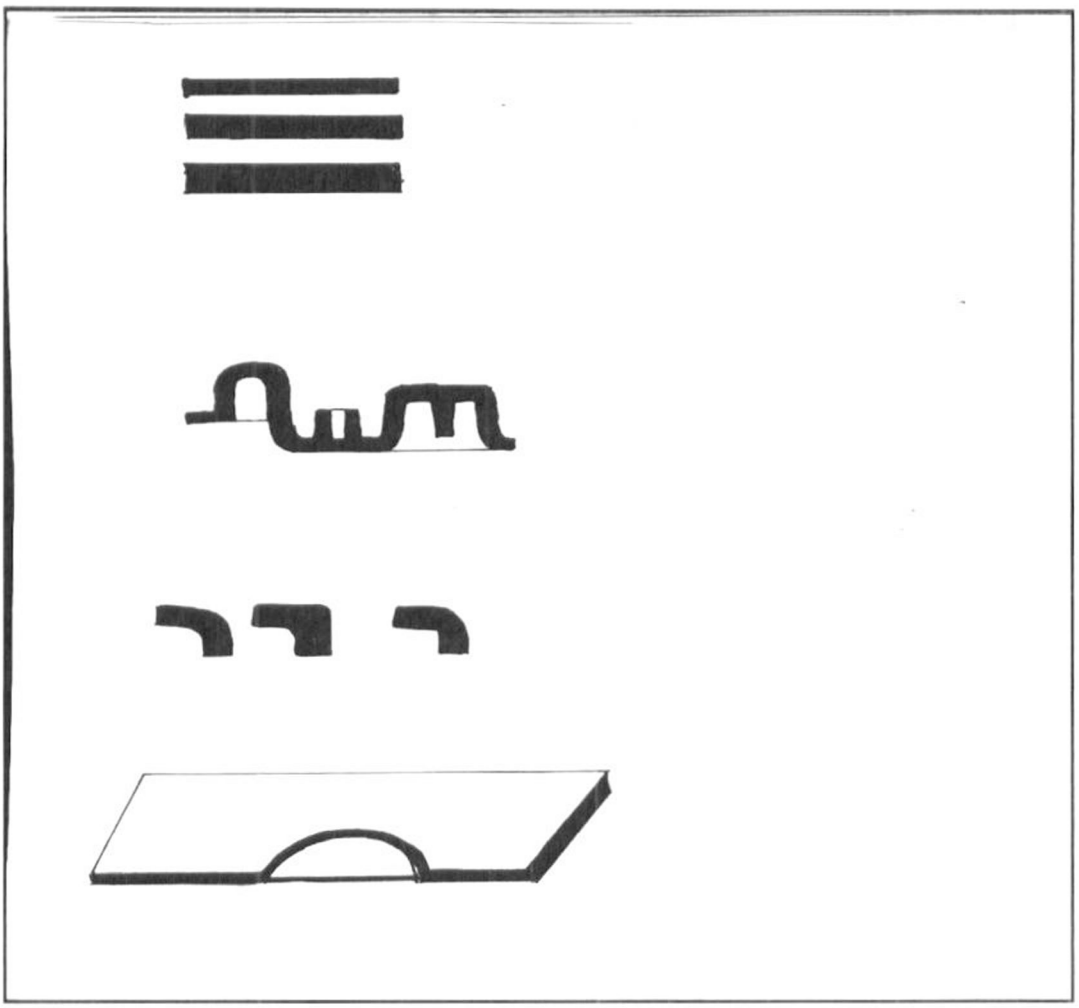

Azami Sağlamlık Tasarımı

- ... Federler- federler takviye için yerleştirilir ve çeliğe karşı büyük avantaş sağlarlar
- ... Federlerin çizgiye oturtulması-resimde görüldüğü gibi çöküntü saklanabilir
- ... Feder Geometrisi-görünür yüzeylerde feder baz kalınlığı parça kalınlığının en fazla % 75 i kadar olmalıdır, görünmiyen yüzeylerde kalınlık parça kalınlığı kadar olabilir
- ... Bos Geometrisi-cıvata ve somun oturtulan boslar montaj kolaylığı sağlar. Tavsiye edilen derinlik ve radyus değerleri reimde gösterilmiştir.

... Sağlamlığı artırmak için kenarlarda flanş şekli tavsiye edilir
... Üretimi hızlandırmak için flanş yerine kenarların kalınlaştırılması tercih edilirİki parçalı konstruksiyonlar iki ayrı parçanın yapıştırılmasıyla oluşurlar. Bu şekilde de salamlık artırılabilir

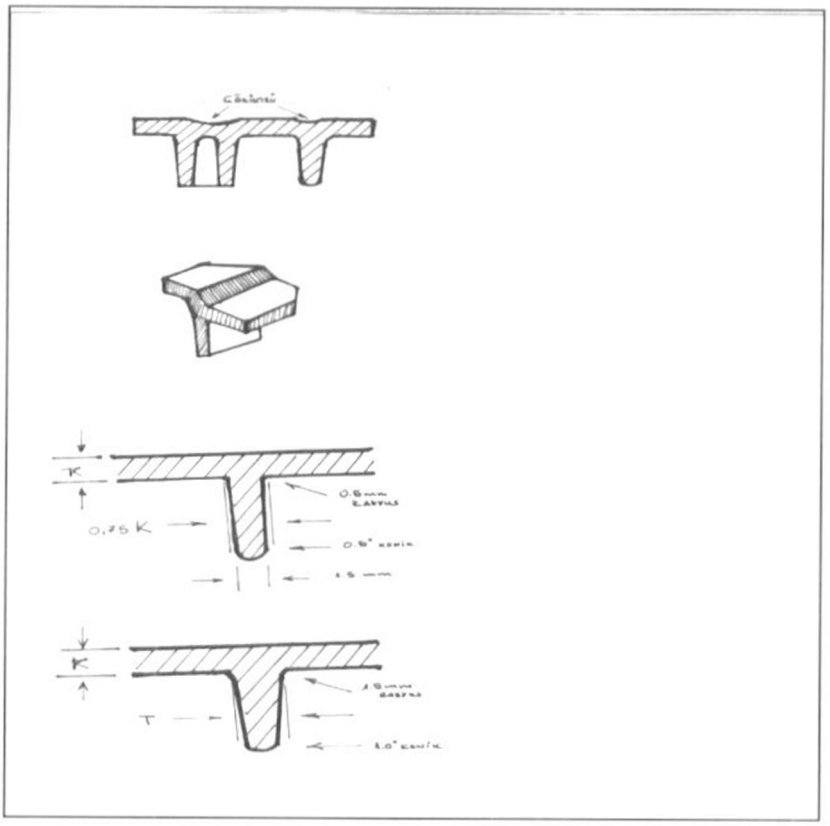

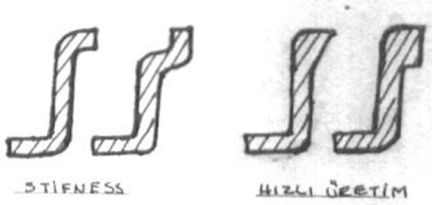

STİFNESS HIZLI ÜRETİM

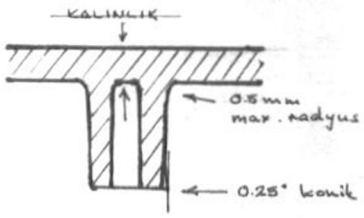

CLASS A

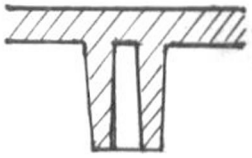

YÜKSEK DAYANIKLILIK

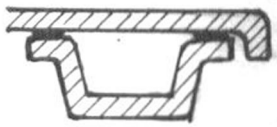

İKİ PARÇA

Kritik Ölçüler Kontrolü İçin Dizayn Uyarıları:

- Toleranslar – SMC-BMC için geçerli toleranslar ölçülerin tekrarlanabilirliğini etkilemektedir
- Presler- pres üreticileri arasında pres paralelliği toleranslarında farklılıklar bulunmaktadır
- Kalıp – kalıp toleransları +/- 0.25 mm ye kadar çıkabilmektedir
- Malzeme- malzeme reaksiyon çekmelerinde toleransı da hesaba katmak gerekir
- Baskı Tarihleri- kalıpta tarih damgası yapıştırılan parçalar için çok önemlidir.

PHENYLETHYNYL TERMINATED IMIDE (PETI) COMPOSITES MADE BY HIGH TEMPERATURE VARTM

Sayata Ghose[1], Roberto J. Cano[2], Kent A. Watson[1], Sean M. Britton[2], Brian J. Jensen[2], John W. Connell[2], Helen M. Herring[3] and Quentin J. Linberry[4]

[1]National Institute of Aerospace, Hampton, VA 23666-6147

[2]NASA Langley Research Center, Hampton, VA 23681-2199

[3]Lockheed Martin Engineering & Sciences Company, Hampton, VA 23666

[4]NASA GSRP at Western Kentucky University, Bowling Green, KY 42101

sayata.ghose-1@nasa.gov

Abstract

The use of composites as primary structures on aerospace vehicles has increased dramatically over the past decade. As these advanced structures increase in size and complexity, their production costs have grown significantly. A major contributor to these manufacturing costs is the requirement of elevated pressures, during high temperature processing, to create fully consolidated composite parts. Recently, NASA Langley has licensed a series of low viscosity Phenyl Ethynyl Terminated Imide, PETI, oligomers that possess a wide processing window to allow for Resin Transfer Molding, RTM, processing. These resins, PETI-8 and PETI-330, demonstrate void fractions of ~1% under elevated pressure consolidation. However, when used with a standardized thermal curing cycle in a High Temperature Vacuum Assisted RTM (HT-VARTM) process, they display undesirable void contents in excess of 7%. A thermogravimetric-mass spectroscopic study was conducted to determine the source of volatiles leading to high porosity. It was determined that under the thermal cycles used for laminate fabrication, the phenylethynyl endcap underwent degradation leading to volatile evolution. Modifications to the processing cycle used in the laminate fabrication have reduced the void content significantly (typically less than 3%) for carbon fiber biaxially woven fabric. For carbon fiber uniaxial fabric, void contents of less than 2% have been obtained using both PETI-8 and PETI-330. The resins were infused into carbon fiber preforms at

260°C and cured between 316°C and 371°C. Photomicrographs of the panels were taken and void contents were determined by acid digestion. Mechanical properties of the panels were determined at both room and elevated temperatures. These include short beam shear and flexure tests. The results of this work are presented herein.

Keywords: phenylethynyl terminated imides, VARTM, voids, acid digestion, mechanical properties

NANO-TAKVİYELİ MALZEME ÜRETİMİ İÇİN YENİ BİR YÖNTEM

A NOVEL METHOD FOR PRODUCTION OF A NANO-REINFORCED MATERIAL

İdris KAYNAK

Dumlupınar University, Faculty of Technology, Department of Manufacturing Engineering
43500, Simav / Kütahya, Turkey

idriskaynak@dpu.edu.tr

Bu yenilikçi çalışmanın amacı, polyamid, cam elyaf ve nano-malzemelerin birleştiril-mesi yoluyla tercihinize göre çelik yada seramik malzemelerin fiziksel özelliklerine sahip bir nano-takviyeli malzeme gerçekleştirmektir. Fiber oryantasyon ve dağılımları kapatma basıncı dikkate alınarak farklı reolojik özellikleri nedeniyle dolum aşamalarında sayısal analiz programıyla incelenmiştir. Lif oryantasyon akış analizi Moldflow/MPI-Fiber, yazılım paketi kullanılarak yapıldı. Poliamid kompozit ürünler (ASTM- D 638) standardı ile başarılı olarak üretildi ve mikroyapısal gözlemler elektronik mikroskop ile elde edilmiştir. Elastikiyet modülü ve çekme test sonuçlarının laboratuvar bulguları, 21 GPa ve 235 MPa olarak sırasıyla elde edildi. Dolayısıyla sonuçlara göre patent başvurusu yapıldı. Elde edilen laboratuvar sonuçlarına göre, düşük alaşımlı karbon çeliğinin akma noktasına ulaşılmıştır. Patentin uluslararası başvuru no (PCT/IB2008/053662) ve uluslararası yayın no WO 2010/029387 A1'dir.

Abstract

The objective of the present innovative study is to realize a nano-reinforced material having physical properties of steel or ceramics materials according to preference by means of polyamide, fiber glass and nano-combining materials. Because of different rheological properties of the fiber orientation and in distributions to considering the closing pressure are investigated as well as the filling stages by the numerical software analysis. The flow analysis of fiber orientation was performed utilizing a

Moldflow/MPI-Fiber software package. The polyamide composite products were successfully produced (ASTM-D 638) and the micro-structural observations were obtained by electronic microscope. The modulus of elasticity and tensile test results were obtained in the laboratory features, 21GPa and 235MPa, respectively. Consequently, according to results the patent application was made. According to obtained laboratory results, were reached to yielding point of low alloy carbon steel's. The international application number of patent is (PCT/IB2008/053662) and international publication number is WO 2010/029387 A1.

I. Introduction

Fibers of rayon, glass, nylon and carbon are commonly used for polymer composites [1] to change rheological properties, processibility and product quality by controlling fiber orientation, distribution and dispersion [2]. The mechanical properties of components made of short fiber reinforced composites, generally obtained by injection [3] compression moldings (ICM) are strongly linked to flow-induced alignment of fiber orientation in composite materials. Therefore, it is of great importance to be able to verify the results of real-time manufacturing process simulations can be obtained by commercial software's. As mechanical properties of short fiber reinforced thermoplastic injected components depend on flow-induced short fiber orientation (FI-SFO), there is considerable interest in validating and improving models which link the flow field and fiber orientations to mechanical properties. Most polymers can be injection molded, including fiber reinforced and engineering thermoplastics, thermosetting polymers and liquid crystal polymers.
Most observations in injected parts show two skin layers with preferential orientation parallel to the flow direction, and a core region with orientation perpendicular to the flow and in the plane of the part (see a review in Ref. [4]). It is known that in a pure shear flow, fibers orient mainly in the flow direction, whereas in extensional flows, they orient in the direction of extension. Most injected parts have a nearly constant thickness, which is much lower than the other dimensions. Therefore, shear deformations are dominant, and this explains the skin layers. A divergent flow is responsible for the core layer. This happens at the gate that is at the junction between the feeding channel and the cavity itself, whose cross-section is larger than that of the channel [5].

In the present study, the gate channel was created as fiber bundle in the circle throughout the one way direction to the laterally mold cavity. The present study concerns firstly the observation and quantification of fiber orientation (FO) in a rectangular plaque (ASTM D638) with adjustable thickness and molded with 30 and 40 wt% short glass fiber reinforced in polyamide.

II. Materials And Methods

A molded part can have different degrees and directions of short fiber orientation (SFO) state and it should be expected that non-uniform structure will give rise to dissimilar mechanical properties at every point in the part. Therefore, it is desirable to understand the way flow inducement during mold filling influences fiber orientation states. In this possible scenario, predictable the flow-induced orientation of the fibers at every single point will play so important role of a structural state variable. Therefore, the general case is needed, concise, quantitatively and unambiguously determination of fiber orientation solid states. The main field of the objective of the study is to use tensor descriptions, which meets the above requirements, to characterize and fiber orientation prediction for three dimension injection-compression molded parts during polymer composite flow. These types of quantitative predictions of strands fiber orientation will be provided better ability to control the microstructure and, consequently, the mechanical properties of the injection-compression molded (ICM) parts [6]. An alternate method of averaging the properties of aligned fiber is volume averaging [7]. Let $n(i,t,d)$ be the orientation density function, defined as the fraction of fibers oriented at i,t and d. Here i,t,d are the Eulerian angles defined in the below in Fig. 2. The volume average, $< V_{ij} >$, of a second order tensor, V_{ij} is given by*

$$< V_{ij} > = < E_{mi} E_{nj} > V_{mn}, \text{ and where,}$$

$$?E_{mi} E_{nj} A @ \int_0^{s} \int_0^{\frac{s}{2}} \int_0^{s} n(i,t,d) \sin t \, \hat{E}_{mi} E_{nj} \, di \, dt \, dd$$

$< >$ this represents the average property and the E_{ij} are the components of the Eulerian rotation matrix as shown in Fig.2. V_{mn} represents the properties of an aligned short fiber composite and $<V_{ij}>$ represents the average of that property over all directions weighted by the orientation density function.

*Whenever Cartesian tensor notation is used, summation over the repeated indices is implied.

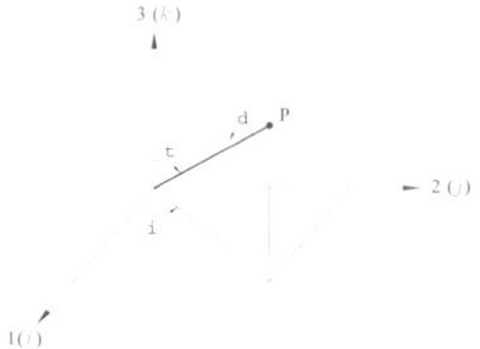

Figure 2. The orientation of a single axis-symmetric particle can be described by three components of the Eulerian rotation matrix for following i, t, d , rotations around the (i, j, k) axes [8].

Suppose that each fiber is an axis-symmetric particle, like cylinder shown in fig.2. The orientation such a particle can be described by three angles or by a unite vector p directed along the particle axis. These two description are simply related,

$$P_1 = \sin\theta \cos\varphi , \qquad P_2 = \sin\theta \sin\varphi , \qquad P_3 = \cos\theta$$

where (P_1, P_2, P_3) are the Cartesian components of P. The choice of direction for p is arbitrary, since the "head" of the particle is identical to its "tail". Hence, any description of the particles' orientation must be unchanged if one makes the substitution [9]. The analysis focused on a single particle and the motion of a single rigid ellipsoidal particle immersed in a viscous Newtonian liquid was solved by Jeffery in 1922. His main study of the problem solution about is the velocity of the fluid surrounding the particle. At the inertia terms, Navier-Stokes equations were neglected and the boundary conditions were no slip on the surface of the particles, the local fluid velocity and the bulk velocity at distance far away from the particle are equal. The stresses on the surface of the particle can then be obtained from the gradients of the velocity field. [10].

The injection molding ability of short glass fiber reinforced polyamide granule was injected in to the molding cavity profile of the tensile testing of plastics standard ASTM D 638.The injection moldable materials used polyamide pellets which are BASF company products of the trade name Ultramid, PA. The short glass fibers (chopped strands) reinforced is compatible with polyamide because of the injection molding process of the melting plastics flow is impregnation process. The short glass fibers (SGF) are produced by Cam Elyaf Inc, in Izmit, TURKEY. The short glass fibers diameter is 10-13 μm and the length of SGF is 3-4,75mm [6].

III. Results

The metallographic sample is used for optical microscope. From left to right for each peace took three optical views as left side, middle side and right side. As in the scene below the Figure 5, the injection molding material is prepared for the electronic microscope (LUCIA 4.1, Nikon) sample and from every piece of rectangular cross section surface took clear views. These kind of clear views are chosen two side of the mold wall and also in the middle of the flow how the short glass fiber orientations (SGFO) is distributed in the flow directions. These methods were implemented for Figure 5, than two piece of injection molding material used the testing for mechanical properties. The mechanical properties is determined by the molding material with the (SHIMADZU, AG – 50kNG) universal testing machine.
In the figure 3, can be seen two piece of injection molding materials, the mold was created one way flow direction.The tensile test graphics created as seen in the figure 4.

Figure 3. Injections molding material for test sample standard ASTM D 638 and the tensile test sample material after the ultimate tensile test are seen.

The steel standard of TSE (Institute of Turkey Standard) called Fe-37-2, which is Germany DIN norm is St-37-2, and the yield point is 235MPa. The modulus of elasticity and tensile test results were obtained in the laboratory features, 21GPa and 235MPa, respectively. That point of the view we should look at the compression of the mold part pressure is 100 bar (10MPa) which is good enough. And also cycle time 15 seconds may be little bit longer time 2 or 3 seconds under the compression the mold but I try to create more convenient short glass fiber orientation (distribution) in the polymer matrix material.
As a result, the patent application and material's specific gravity is significant, according to the low alloy steel (St-37), and has reached yield point of low alloy carbon steel.

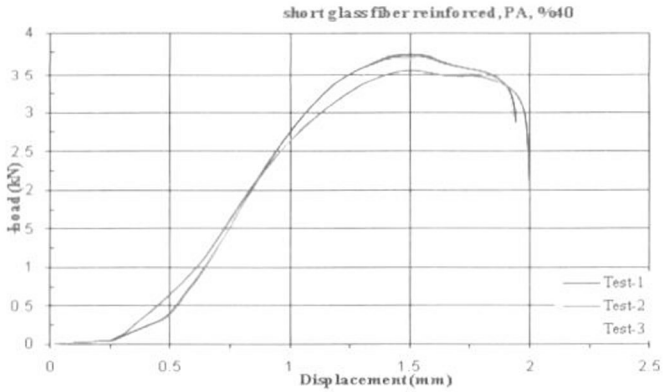

Figure 4. Short glass fiber reinforced 40% in the polymer matrix test result graphics.

Figure 5. Optical microscope sample FO distributions are illustrated in figure 6.

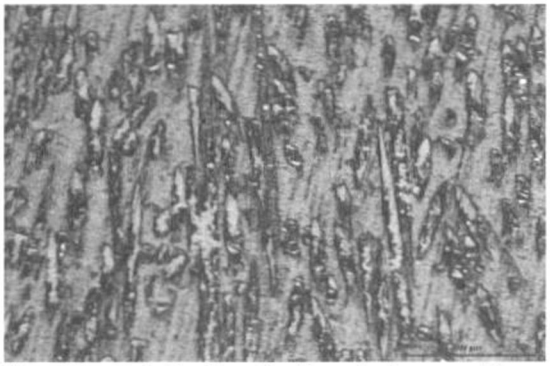

Figure 6. SGFO can be seen in the flow direction of polymer matrix composite.

References

[1] E. Kissa, Dispersions: Characterization, Testing and Measurement, Marcel Dekker, New York, (1999)

[2] M. Yamanoi, J. Maia, T. Kwak, "Analysis of rheological properties of fibre suspensions in a Newtonian fluid by direct fibre simulation" J. of Non-Newtonian Fluid Mechanics, 165, pp. 1064-1071, (2010)

[3] F. Cosmi, A. Bernasconi, N. Sodini "Phase contrast micro-tomography and morphological analysis of a short carbon" Composites Science and Technology, doi:10.1016/j.compscitech.2010.09.016, (2010)

[4] Papathanasiou TD. , "Flow-induced alignment in injection molding of fiber reinfor- ced polymer composites", In: Papathanasiou TD, Guell DC, Editors. Flow-induced alignment in composite materials, Cambridge: Woodhead Publishing Ltd;p. 113–65, (1997)

[5] Michel Vincent, T. Giroud, A. Clarke, C. Eberhardt, "Description and modeling of fiber orientation in injection molding of fiber reinforced thermoplastics" Polymer 46, pp. 6719–6725, (2005)

[6] İ. Kaynak, "Fiber orientation prediction for 3D injection and compression molded parts" Ph.D. Dissertation, Dokuz Eylul University, (2005)

[7] R.L. McCullough, Anisotropic elastic behavior of crystalline polymers, in: Treatise on Materials Science and Technology, Vol.10, Part B, ed. J.M. Schultz, Academic Press, New York, pp.453-540, (1977)

[8]S.G. Advani, "Prediction of fiber orientation during processing of short fiber composites, Ph.D.Dissertation, University of Illinois at Urbana-Champaign. (1987)

[9] S.G. Advani, Flow and Rheology in Polymer Composites Manufacturing, Elsevier, pp. 147-202, (1994)

[10]Chung, D. H. & Kwon, T. H. Fiber orientation in the processing of polymer composites. Korea-Australia Rheology Journal, 14, 4, December, 175-188, (2002)

VAKUM YARDIMLI REÇİNE TRANSFER KALIPLAMA YÖNTEMİ KULLANARAK HİBRİT POLİMER NANOKOMPOZİTLERİN ÜRETİMİ

FABRICATION OF HYBRID POLYMER NANOCOMPOSITES USING VACUUM ASSISTED TRANSFER MOLDING

Volkan ESKİZEYBEK, Ahmet AVCI

Selçuk Üniversitesi Makine Mühendisliği Bölümü, Selçuklu, Konya, 42075,

veskizeybek@selcuk.edu.tr, aavci@selcuk.edu.tr

Özet

Cam fiber ile takviye edilmiş polimer kompozitler (CFTP) sahip oldukları iyi mekanik ve diğer fiziksel özellikleri nedeniyle yapısal uygulamalarda sıkça kullanılmaktadır. Nanoteknoloji alanında yaşanan gelişmeler ile özellikle karbon nanotüp (KNT) gibi geleneksel yapılara göre oldukça yüksek mekanik özelliklere sahip nanoparçaçıkların CFTP içerisine katılmak suretiyle, bu kompozitlerde daha iyi mekanik özellikler elde edileceği fikrini gündeme getirmiştir. Ancak bu fikrin hayata geçirilmesini kısıtlayan en önemli etkenler polimer içerisindeki nanoparçacık miktarı ve nanoparçacıkların polimer içeriside homojen dağıtılabilmektir. Bu amaçla katılacak nanoparçacıkların polimer içerisinde daha iyi dağıtılabilmesi için nanoparçacıkların uygun kimyasal gruplar ile fonsiyonelleştirilmesi, nanoparçacıkların polimer içerisindeki dağılımını arttıracaktır. Bu çalışmada, içerisine ağırlıkça farklı oranlarda KNT ilave edilmiş epoksi reçinesinden vakum yardımlı reçine transfer yöntemi kullanılarak tabakalı cam fiber takviyeli hibrit nanokompozit üretilmeye çalışılmış ve bu yöntemin avantajları ve dezavantajları tartışılmıştır.

Abstract

Due to their good mechanical and other physical properties, glass fiber reinforced polymers (GFRP) are widely used in many structural applications. An idea occurred by means of developments in nanotechnology like adding nanoparticles, especially carbon nanotubes (CNTs) which have very good mechanical properties according to traditional structures, to obtain better mechanical properties in those of the GFRP. But, the amount of the nanoparticles in polymer and dispersing of those nanoparticles into matrix homogenously are the limiting factors of this idea comes true. To increase the homogeneity of the nanoparticles in polymer, suitable functional groups can be used. In this study, CNTs are added into epoxy resin in different amounts to produce laminated GFRP hybrid nanocomposites using vacuum assisted resin transfer molding. Advantages and disadvantages of the process is discussed after production

ÜRETİM TEKNOLOJİLERİ II / PRODUCTION TECHNOLOGIES II

KOMPOZİT MALZEMELERİN TASARIMI, ANALİZİ VE KARAKTERİZASYONU I / COMPOSITE MATERIALS DESIGN, ANALYSIS AND CHARACTERIZATION I

NEW DEVELOPMENTS IN RUBBER REINFORCEMENT

Liliane Bokobza

E.S.P.C.I., Laboratoire PPMD, 10 rue Vauquelin, 75231 Paris Cedex, France
Liliane.Bokobza@espci.fr

Abstract

The mechanical reinforcement imparted by multiwall carbon nanotubes (MWNTs) to elastomeric matrices is analyzed and compared to that provided by conventional fillers. When incorporated into insulating polymeric media, carbon nanotubes provide electrical conduction, at a much lower content than carbon blacks. The extent of property improvement obtained with MWNTs is attributed to their high aspect ratio and to their state of dispersion within the host matrix.

1. Introduction

Elastomers require, in most applications to be reinforced by fillers in order to improve their mechanical properties. Carbon black and silica have been used for a long time in the rubber industry to prepare composites with greatly improved properties such as strength, stiffness and wear resistance. These conventional fillers must be used at high loading levels to impart to the material the desired properties. The state of filler dispersion and orientation in the matrix, the size and aspect ratio of the particles as well as the interfacial interactions between the organic and inorganic phases have been shown to be crucial parameters in the extent of property improvement[1,2].

The last few years have seen the extensive use of nanoparticles with large surface area allowing to achieve the required mechanical properties at much lower filler loadings. Nanometer-scale particles including spherical particles such as silica or titanium dioxide generated in situ by the sol-gel process[3-5], have been shown to significantly enhance the physical and mechanical properties of rubber matrices. On the other hand, alternative fillers with high aspect ratio such as layered silicates[6], carbon[7] or clay fibers[8], single-wall or multiwall carbon nanotubes[9,10] often bring, besides an improvement in mechanical response of the material, other interesting properties such as gas barrier, fire resistance or thermal and electrical conductivities.

The potential of carbon nanotubes (CNTs) as reinforcing fillers for polymeric matrices has been immediately recognized after their first observation in 1991. Carbon nanotubes consist of folded graphene layers with cylindrical hexagonal lattice structure. As a result of this unique arrangement, they display exceptional stiffness and strength and remarkable thermal and electrical properties, which make them ideal candidates for the design of advanced materials. These exceptional properties are expected to impart major enhancements in various properties of polymer composites at relatively low filler loadings (<10 wt.%)[11,12].

The reported exceptional properties have motivated considerable interest in the development of nanotube-based polymer composites. But although most efforts have been devoted to the use of carbon nanotubes in glassy polymers, some studies have reported strong reinforcing effects of CNTs in elastomeric matrices such as butyl [13], natural [10,14-17] and styrene-butadiene rubbers [18,19] as well as ethylene-propylene-diene terpolymer[20]. Nevertheless, the resulting composites do not display their theoretical potential because carbon nanotubes tend to bundle together which inhibits their dispersion in the polymer matrix. All the results obtained by incorporation of CNTs in hydrocarbon rubbers remain far below the expected values and factors such as poor dispersion, weak interfacial bonding, and degradation of the CNTs during processing are often cited to explain the discrepancy between experimental and predicted results.

This paper is intended to review some recent advances in processing and characterization of elastomers filled with multiwall carbon nanotubes (MWNTs). We have investigated the effect of nanotube loading on mechanical and electrical properties of three different sulfur-cured hydrocarbon rubbers : natural (NR), styrene-butadiene (SBR) and ethylene-propylene-diene (EPDM) rubbers. All the composites were prepared by solution blending using a sonication process.

2. Experimental

2.1. Materials

Multiwall carbon nanotubes (MWNTs) were purchased from Nanocyl S.A. (Belgium). In this study, we have used the Nanocyl 7000 series (purity: 90%) produced via the catalytic carbon vapor deposition process without any further purification. Their average diameter and length are around 10 nm and 1.5 μm respectively and their surface area between 250 and 300 $m^2.g^{-1}$. Natural rubber (NR) and styrene-butadiene copolymer (SBR) were supplied by Formix (Orléans, France). Styrene-butadiene rubber (Buna VSL 5025-0 from Bayer) contains 25 wt% of

styrene unit and 50 wt% of vinyl configurations. Ethylene-propylene-diene rubber (EPDM) was supplied by ExxonMobil Chemical under the trade name Vistalon 5601). It contains 68.5 wt% of ethylene, 5 wt% of diene and a Mooney viscosity MU at (1+4) at 125°C of 72. Their formulation is described in Table 1.

Table 1. Formulation of the different composites (all the ingredients are expressed in phr = parts by weight per hundred parts of rubber).

Ingredients (phr)	NR composites	SBR composites	EPDM composites
Rubber	100	100	100
Zinc oxide	3	1.82	
Stearic acid	2	1.1	
Sulfur	1.5	1.1	1
Cyclohexylbenzothiazole sulfenamide	1.5	1.3	
Diphenyl guanidine	0	1.45	
2-mercaptobenzothiazole			0.8
Zinc dibenzyldithiocarbamate			0.8

2.2. Composite processing

Different approaches have been used to optimize the dispersion of CNTs in the polymeric medium. Composites can be prepared by different techniques including in situ polymerization, solution mixing, surfactant-assisted processing and melt compounding. On the other hand, introduction of functional groups on the nanotube surface has also been used to improve adhesion at the polymer-filler interface and also dispersibility. But these treatments affect the chemical nature of the tube surface and can shorten their length.

In this work, solution mixing which is one of the most common methods, has been used for the preparation of the various composites. The general protocol is to mix both components in a suitable solvent and evaporate the latter before proceeding to the cross-linking process and film formation. The most efficient dispersion of the nanotubes in a solvent is achieved by tip sonication with sonication conditions determined in such a way not to degrade the nanotubes[21].

An appropriate amount of MWNTs was dispersed into cyclohexane (0.1 mg/ml) by sonicating the suspension for 30 min using a Vibra-Cell VCX 500 operating at 40% amplitude with on and off cycles respectively equal to 4 and 2 seconds. Cyclohexane

was used to disperse the nanotubes because it can also dissolve natural rubber and is less dangerous than toluene which is a good solvent for rubbers.

The gum containing the rubber and all the ingredients of formulation was mixed separately in cyclohexane under magnetic stirring until complete dissolution then mixed with the MWNTs dispersion. The mix of polymer and MWNTs dispersions is stirred until evaporation of the major part of cyclohexane then put under vacuum at 50°C for one day for total removal of remaining solvent.

The unfilled and filled samples were then cured into plaques at 170°C during 10 min under a pressure of 150 bar in a standard hot press for NR and SBR, at 140°C during 30 min under 150 bar for EPDM. The resulting films were around 300 □m thick.

2.3. Characterization techniques

Electrical resistivity measurements were determined on samples of 10 „ 20 „ 0.2 mm^3 by measuring their resistance on a high resistance meter (Keithley 6517A) between two conductive rubber electrodes with an alternative voltage of 1 V. This alternative voltage is needed to avoid a background current effect.

Atomic force microscopy (AFM) images were recorded by using a commercial instrument (Veeco, Digital Instruments D3100) in tapping mode. Height (sample topography) and phase images were recorded simultaneously at the resonance of the cantilever and the scan dimension varied between 3 and 20 □m.

Strips of unfilled and filled elastomers were used in the uniaxial elongation experiments carried out to obtain the stress-strain curves at equilibrium[22]. The nominal stress □, was calculated from □ = f / A, where f is the elastic force and A is the undeformed cross-sectional area.

The dynamic properties of the vulcanizates were measured by means of a Anton Paar Rheometer at 1Hz sinusoidal oscillation, using disc specimens with thicknesses of 2mm, diameters of 8 mm, operated in a shear mode.

3. Results and discussion

3.1. Electrical conductivity

As already mentioned, the sample preparation process has a strong impact on the composite properties and especially on electrical properties. After processing, the electrical conductivity is systematically measured before proceeding to any other type of investigation. Actually, the use of nanoscale conducting fillers such as carbon nanotubes has proven to be effective in reducing the filler content required to achieve the electrical percolation threshold. Above a certain amount of conductive

particles, called the percolation threshold, an interconnecting filler network is formed which results in the sharp drop of the electrical resistance of the composites.

The dependence of volume resistivity on the nanotube content is reported in Figure 1. For the three different matrices, it is seen to be around 0.5 phr (0.2 vol %) which is much lower than that already reported for this type of polymers[10,15,16,18,19,22]. This percolation threshold is also much lower than those of composites containing conventional microscale conducting fillers like carbon black or graphite where the amount of particles needs to be as high as 10-50 wt % [22]. This major attribute of carbon nanotubes to form a conducting network at a very low loading content is due to their intrinsically high conductivity and high aspect ratio. Nevertheless, the improvement in electrical conductivity obtained in this present study with regard to previous results, indicates that our processing conditions using sonication method yield a better nanotube dispersion within the elastomeric matrix. Atomic force microscopy (AFM) investigation using tapping mode and phase imaging performed on a SBR/MWNTs composite reveals a pretty nice dispersion (Figure 2). There is a good connection between the topography and phase images which show unambiguously nanotubes appearing in bright.

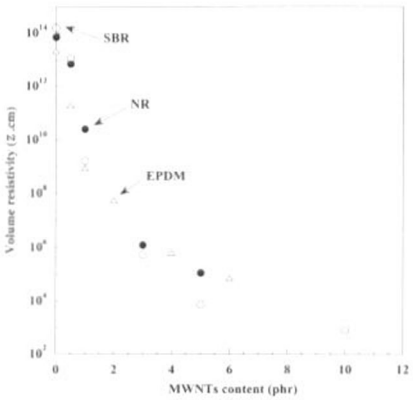

Figure 1. Dependence of volume resistivity on carbon nanotube loading for NR, SBR and EPDM composites.

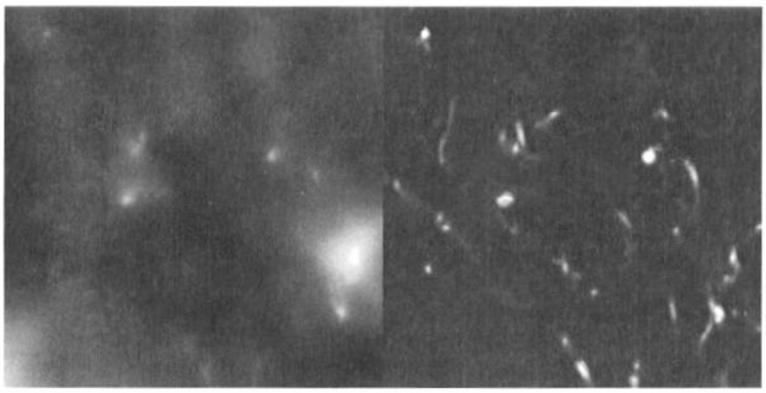

0 3 m 0 3 m

Figure 2. Topography (left) and phase (right) images of a SBR filled with 10 phr of MWNTs.

3.2. Mechanical properties

The potential of CNTs as reinforcing fillers for elastomeric matrices can be evidenced in the stress-strain curves of the MWNts/SBR composites for example, which exhibit, with regard to the unfilled matrix, considerable improvements in stiffness as revealed by the linear increase in the elastic modulus with the nanotube loading (Figure 3 left). When compared with the unfilled elastomers, the elastic and tensile moduli of the composite filled with 10 phr of MWNTs are seen to increase by almost 1300 and 700% respectively. Such improvement results from the anisometry of the filler structures, their ability to align in the direction of strain as well as their state of dispersion in the host matrix.

The effect of the high aspect ratio can be evidenced by fitting the experimental results to the Halpin-Tsai model[23] intended to predict the mechanical properties of fibre reinforced composites. This model, leads, for aligned fibre composites and in conditions where the fibre modulus is much higher than the modulus, E_0, of the unfilled polymer, the following expression of the modulus, E, of the composite :

$E = E_0 (1 + 2f\square) / (1 - \square)$

f and being the aspect ratio and volume fraction of filler, respectively.

An aspect ratio of 100 is obtained by fitting the experimental results to the Halpin-Tsai model (Figure 3 right). This value, lower than that expected from the average

dimension of the MWNTs but much higher than that previously published for hydrocarbon/MWNTs composites[12,19], indicates that our solution mixing method by a simple sonication is effective in dispersing the nanotubes without the need of surfactants or other chemical treatments such as nanotube surface functionalization.

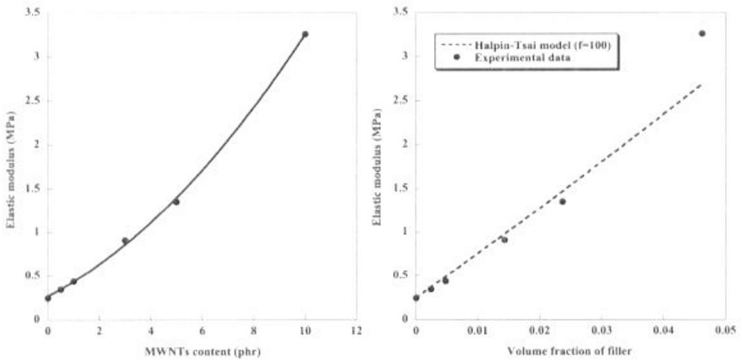

Figure 3. Dependence of the elastic modulus on the nanotube loading (left), versus filler volume fraction for SBR/MWNTs composites and comparison with the prediction of the Halpin-Tsai model using a filler aspect ratio of 100 (right).

Filled elastomers have the specific ability to dissipate an important part of mechanical energy during deformation. At small strains (typically for shear strains below 100%), those materials exhibit a non-linear viscoelastic behavior , known as the "Payne effect" and characterized by a drop in the elastic modulus G' when the shear strain amplitude increases.

The Payne effect in composites filled with conventional fillers (carbon black or silica) has been the subject of numerous studies on both experimental and theoretical aspects[24-27] but its origin is still controversial. The most commonly accepted picture is the breakdown of a filler network formed by filler-filler interactions. The percolated network is progressively broken by increasing the strain amplitude.

Figure 4a displays the strain dependence of the storage modulus of the unfilled NR and of MWNTs-filled composites. While the unfilled elastomer does not display any change in the storage modulus with strain amplitude, at least in the investigated strain domain, the observed behaviors for filled compounds are similar to what was

mentioned in the literature for carbon-black filled rubbers, that is an increase in amplitude of the Payne effect with the amount of reinforcing particles, because the linear part of the storage typically below 0.1% strain strongly increases with the filler loading. But as shown in Figure 4a, a Payne effect is observed till 0.5 phr while much larger amounts of carbon black are required to give rise to a storage modulus drop with the strain amplitude[28].

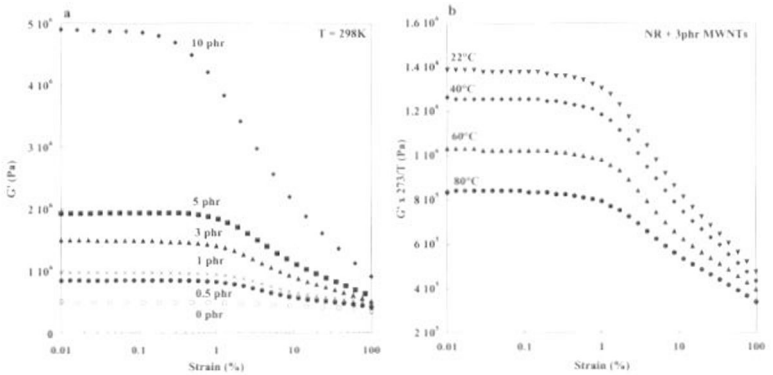

Figure 4. Strain dependence of the storage modulus of unfilled NR and of MWNTs/NR composites at room temperature (a) and temperature dependence of the storage modulus for NR filled with 3 phr of MWNTs (b).

In the case of an unfilled rubber network, the modulus should increase proportionally with temperature because of its entropic nature. For all the filled systems, the modulus values should then be corrected by the entropic factor 273/T, in order to get rid of the modulus dependence of the rubber part due to temperature. As a typical exemple, the temperature dependence of the storage modulus is shown in Figure 4b for the 3 phr MWNTs/NR composite. As already observed in conventional composites, the amplitude of the Payne effect decreases with increasing temperature which is opposite to the entropic variation characteristic of the unfilled network. The decrease of the Payne effect results from a weakening of filler-filler interactions by raising the temperature.

The well-known phenomenon called stress-softening or Mullins Effect[29], observed at high extensions and characterized by a pronounced lowering in the stress during a

second extension, is also present in nanotube-filled composites. Figure 5 compares the first and second stretchings performed on a unfilled SBR and on a SBR composite filled with 5phr of MWNTs. While the pure polymer does not display any significant softening, the carbon nanotube-composite shows a strong reduction in stress when extended a second time.

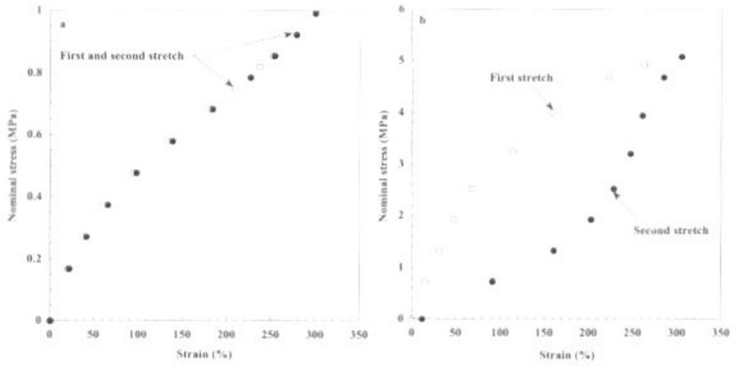

Figure 5. Stress-softening effects for unfilled SBR (a) and for SBR/ 5phr MWNTs composite (b).

Conclusion

Carbon nanotubes really appear to be the ultimate filler for elastomers since they impart unprecedented levels of reinforcement to the rubbery matrices. It is due to the high aspect ratio and the relatively good state of dispersion. Another major attribute is to allow the formation of conductive polymers with tiny amounts of nanotubes.

References

[1] Bokobza L.: The reinforcement of elastomeric networks by fillers. Macromolecular Materials and Engineering, **289,** 607-621 (2004).

[2] Bokobza L.: Elastomeric Composites. I. Silicone composites. Journal of Applied Polymer Science, **93,** 2095-2104 (2004).

[3] McCarthy D.W., Mark J.E., Schaffer D.W.: Synthesis, structure, and properties of hybrid organic-inorganic composites based on polysiloxanes. I. Poly(dimethylsiloxane) elastomers containing silica. Journal of Polymer Science: Part B: Polymer Physics, **36,**1167-1189 (1998).

[4] Kohjiya S., Murakami K., Iio S., Tanahashi T., Ikeda Y.: In situ filling of silica onto "green" natural rubber by the sol-gel process. Rubber Chemistry and Technology, **74,** 16-27 (2001).

[5] Dewimille L., Bresson B., Bokobza L.: Synthesis, structure and morphology of poly(dimethylsiloxane) networks filled with in situ generated silica particles. Polymer, **46,** 4135-4143 (2005).

[6] Arroyo M., López-Manchado M.A., Herrero B.: Organo-montmorillonite as substitute of carbon black in natural rubber compounds. Polymer, **44,** 2447-2453 (2003).

[7] Gauthier C., Chazeau L., Prasse T., Cavaillé J.Y.: Reinforcement effects of vapour grown carbon nanofibres as fillers in rubbery matrices. Composites science and Technology, 65, 335-343 (2005).

[8] Bokobza L, Chauvin J-P.: Reinforcement of natural rubber: use of in situ generated silicas and nanofibres of sepiolite. Polymer, **46,** 4144-4151 (2005).

[9] López-Manchado M.A., Biagiotti J., Valentini, L., Kenny J.M.: Dynamic mechanical and Raman Spectroscopy studies on interactions between single-walled carbon nanotubes and natural rubber. Journal of Applied Polymer Science, **92,** 3394-3400 (2004).

[10] Bokobza L., Kolodziej M.: On the use of carbon nanotubes as reinforcing fillers for elastomeric materials. Polymer International, **55,** 1090-1098 (2006).

[11] Moniruzzaman M., Winey K.I.: Polymer nanocomposites containing carbon nanotubes. Macromolecules, **39,** 5194-5205 (2006).

[12] Bokobza L.: Multiwall carbon nanotube elastomeric composites : A review. Polymer, **48,** 4907-4920 (2007).

[13] Bokobza L., El Bounia N.-E.: Reinforcement effects of multiwall carbon nanotubes in elastomeric matrices/ comparison with other types of fillers. Composite Interfaces, **15,** 9-17 (2008).

[14] Kolodziej M., Bokobza, L., Bruneel J.-L.: Investigations on natural rubber filled with multiwall carbon nanotubes. Composite Interfaces, **14,** 215-228 (2007).

[15] Fakhru'l-Razi A., Atieh M.A., Girun N., Chuah T.G., El-Sadig M., Biak D.R.A.: Effect of multi-wall carbon nanotubes on the mechanical properties of natural rubber. Composite Structures, **75,** 496-500 (2006).

[16] Bhattacharyya S., Sinturel C., Bahloul O., Saboungi M.-L., Thomas S., Salvetat J.-P.: Improving reinforcement of natural rubber by networking of activated nabotubes. Carbon, **46,** 1037-1045 (2008).

[17] Cataldo F., Ursini O., Angelini G.: MWNTs elastomer nanocomposite, Part 1: The addition of MWNTs to a natural rubber-based carbon black-filled rubber compound. Fullerenes, Nanotubes and Carbon Nanostructures, **17,** 38-54 (2009).

[18] Bokobza L., Belin C.: Effect of strain on the properties of a styrene-butadiene rubber filled with multiwall carbon nanotubes. Journal of Applied Polymer Science, **105,** 2054-2061 (2007).

[19] Perez L.D., Zuluaga M.A., Kyu T., Mark J.E., Lopez B.L.: Preparation, characterization, and physical properties of multiwall carbon nanotube/elastomer composites. Polymer Engineering and Science, **49,** 866-874 (2009).

[20] Barroso-Bujans F., Verdejo R., Pérez-Cabero M., Agouram S., RodrÍguez-Ramos I., Guerrero-Ruiz A., López-Manchado M.A.: Effects of functionalized carbon nanotubes in peroxide crosslinking of diene elastomers. European Polymer Journal, **45,** 1017-1023 (2009).

[21] Bokobza L., Rahmani M.: Carbon nanotubes: Exceptional reinforcing fillers for silicone rubbers. Kautschuk Gummi Kunststoffe, 62, 112-117 (2009).

[22] Bokobza L., Rahmani M., Belin C., Bruneel J.-L., El Bounia N.-E.: Blends of carbon blacks and multiwall carbon nanotubes as reinforcing fillers for hydrocarbon rubbers. Journal of Polymer Science: Part B: Polymer Physics, **46,** 1939-1951 (2008).

[23] Halpin J.C.: Stiffness and expansion estimates for oriented short fiber composites. Journal of Composite Materials, 3,732-734 (1969).

[24] M.-J. Wang, Effect of polymer-filler and filler-filler interactions on dynamic properties of filled vulcanizates, Rubber Chemistry and Technology, 71,520-589 (1998)

[25] F. Clément, L. Bokobza and L. Monnerie, Investigation of the Payne effect and its temperature dependence on silica-filled polydimethylsiloxane networks. Part I: Experimental results, Rubber Chemistry and Technology, 78,211-231 (2005)

[26] F. Clément, L. Bokobza and L. Monnerie, Investigation of the Payne effect and its temperature dependence on silica-filled polydimethylsiloxane networks. Part II: Tests of quantitative models, Rubber Chemistry and Technology, 78,232-244 (2005)

[27] J. Ramier, C. Gauthier, L. Chazeau, L. Stelandre and L. Guy, Payne Effect in Silica-Filled Styrene-Butadiene rubber: Influence of Silica Treatment, Journal of Polymer Science: Part B: Polymer Physics, 47,286-298 (2007)

[28] A.R. Payne, The Dynamic Properties of Carbon Black-Loaded Natural Rubber Vulcanizates. Part I., Journal of Applied Polymer Science, VI, 57-63 (1962)

[29] Mullins L.: Softening of rubber by deformation. Rubber Chemistry and Technology, 42,339-362 (1969)

DOĞAL LİF TAKVİYELİ SANDVİÇ YAPILI KOMPOZİTLERİN KARAKTERİZASYONU

CHARACTERIZATION OF NATURAL FIBRE-REINFORCED SANDWICH STRUCTURED COMPOSITES

Levent Önal,

Erciyes Üniversitesi Tekstil Mühendisliği Bölümü

Kayseri/TÜRKİYE

lonal@erciyes.edu.tr

Yekta Karaduman

Bozok Üniversitesi Akdağmadeni Meslek Yüksekokulu

Yozgat/TÜRKİYE

yekta.karaduman@bozok.edu.tr

Özet

Doğal lif takviyeli polimerik kompozitlere ilgi son yıllarda çevresel ve ekonomik nedenlerden dolayı artmıştır. Doğal lif takviyeli kompozit yapıların en önemli avantajı düşük yoğunluklu, ucuz ve ekolojik yönden zararsız olmalarıdır. Sandviç kompozit yapılar ise hafiflikleri ve yüksek mekanik özellikleri ile ilgi çeken malzemelerdir. Bu çalışmada sandviç yapılı doğal lif kompozitlerinin özellikleri incelenmiştir. Bu amaçla takviye malzemesi olarak jüt dokuma kumaşı; reçine olarak ise polyester kullanılarak sandviç yapılı kompozitler üretilmiştir. Kompozit üretim

tekniği olarak vakum infüzyon tekniği kullanılmıştır. Üretilen kompozit yapıların karakterizasyonu yapılmış ve eğilme özellikleri incelenmiştir. Bu kapsamda, jüt kumaş oranı, sodyum hidroksit (NaOH) ön işlemi ve dikiş gibi üretim değişkenlerinin kompozit özelliklerine etkisi incelenmiştir. Çalışma sonucunda doğal lif takviyeli sandviç yapılı kompozitlerin otomotiv ve yat endüstrileri gibi hafif yapısal malzemelerin önemli olduğu alanlarda kullanılabileceği öngörülmüştür.

Abstract

There is a growing attention to natural fiber reinforced polymeric composites in recent years due to economical and environmental reasons. The major advantage of natural fiber reinforced structures is that they are low-weight, cheap and ecologically harmless. Sandwich structures have also attracted great attention because of their low-density and high mechanical properties. In this work, the properties of natural fiber reinforced sandwich structured composites were investigated. For this purpose, sandwich composites with jute fabric as reinforcement material and polyester as resin were produced. Vacuum infusion technique was used for composite production. The structural characterization of natural fibre reinforced sandwich composites and its bending strength was studied. In this scope, the effect of production variables such as jute fabric ratio, sodium hydroxide (NaOH) pretreatment and stitching on composite properties was investigated. It is concluded that natural fiber reinforced sandwich structured composites can be used in such areas where low weight structural components are demanded such as automotive and yacht manufacturing industries.

1. Giriş

Son yıllarda özellikle Avrupa ülkelerinde küresel ısınma tehdidi ile birlikte yaşanan çevresel kaygılar ve buna bağlı uygulanan katı çevre yasaları, malzeme dünyasında büyük değişimler meydana getirmiştir. Bu kapsamda Endüstrinin arayışı petrol bazlı sentetik mühendislik malzemeleri yerine doğal malzemelere yönelmiştir. Malzeme dünyasında yaşanan bu değişimle birlikte polimerik kompozit malzeme üretiminde bugün için en fazla kullanılan cam, karbon, aramid gibi lifler bir takım alanlarda yerini keten, kenevir, kenaf ve jüt gibi sert doğal liflere bırakmaktadır. Doğal lifler çevreye zararsız olmalarının yanında bol ve ucuz malzemelerdir. Doğal liflerden elde edilen kompozitlerin mekanik özellikleri cam, karbon ve aramid destekli kompozitlere nazaran düşük olmasına rağmen hafif olmalarından dolayı özgül mekanik özellikleri (mekanik özellik/yoğunluk) cam lifi kompozitleri ile

yarışabilecek seviyededir. Bu olumlu özellikler doğal lif kompozitlerine olan ilgiyi otomotiv, inşaat ve rekreasyon gibi alanlarda arttırmıştır [1-5].

Jüt lifi, bol üretilmesi ve ucuzluğunun yanında yüksek mekanik özellikler göstermesi bakımından doğal lifler içinde farklı bir yere sahiptir. Jüt lifi tropikal bölgelerde yetişen jüt bitkisinden elde edilen kalın, güçlü ve sert bir liftir. Jüt bitkisi yapısı itibarıyla iki türden oluşur. Bunlar *Corchorus Capillaries L.* (beyaz jüt) ve *Corchorus Olitorus L.* (tossa jüt)'dur. Bugün en çok jüt üretimi gerçekleştiren ülkeler Hindistan ve Bangladeş'tir. Diğer jüt yetiştirici ülkeler ise Çin, Tayland, Nepal, Endonezya, Brezilya, Burma, Peru ve Vietnam'dır [6].

Jüt lifinin avantajları şunlardır:

- Kullanım sırasında çevreye zararsız doğal bir madde olması
- Kullanım ömrü bittikten sonra doğada mikroorganizmalar tarafından biyolojik olarak parçalanabilmesi, dolayısıyla çevre kirliliğine neden olmaması
- Bol miktarda üretilmesi ve ucuz olması
- Yüksek özgül mukavemet ve modül değerleri
- Yoğunluğunun düşük olması
- Boyut stabilitesinin ve sürtünmeye karşı dayanımın yüksek olması
- Yakılıp yok edildiği zaman ortada hiçbir atık madde kalmaması ve oluşan zararlı bileşik miktarının çok az olması
- Makine kısımlarına zarar vermemesi
- Boşluklu yapısı nedeniyle ses absorpsiyon özelliğinin çok iyi olması [7].

Jüt lifinin dezavantajları ise şunlardır:

- Neme karşı ilgisinin yüksek olması
- Küflenme dayanımının az olması [6].
- 170°C 'nin üzerinde mekanik özelliklerinin büyük oranda azalması [8].

Sandviç kompozit yapılar hafiflikleri ve yüksek mekanik özellikleri ile ilgi çeken malzemelerdir. Sandviç yapılar bu olumlu özellikleri nedeniyle bilhassa II. Dünya savaşında uçak üretiminde çok miktarda kullanılmıştır.

Bu çalışmada sandviç yapılı doğal lif kompozitlerinin bazı mekanik özellikleri araştırılmıştır. Bu kapsamda jüt dokuma kumaşı ve gözenekli polyester kumaşı ile

desteklenmiş polyester reçineli kompozitler üretilmiştir. Kompozitler dikişli ve dikişsiz olmak üzere 2 farklı ön şekilden üretilmiştir. Kompozit üretim tekniği olarak vakum infüzyon tekniği kullanılmıştır. Üretilen kompozitlerin 3 noktadan eğilme özellikleri belirlenerek, jüt kumaş oranı, sodyum hidroksit (NaOH) ön işlemi, dikiş gibi üretim değişkenlerinin kompozit özelliklerine etkisi incelenmiştir.

2. Malzeme ve Yöntem

2.1. Malzeme

Numune üretiminde destekleyici olarak bezayağı örgülü jüt dokuma kumaşı (*Hessian Cloth*) ve gözenekli polyester kor kumaşı kullanılmıştır.

Kompozit üretiminde reçine olarak polyester kullanılmıştır. Polyester reçine, sertleştiricisi ve reaksiyon hızlandırıcısı POLIYA firmasından temin edilmiştir. Poliya Polipol 3401 reçinesinin yoğunluğu 1,128g/cm^3'tür. Polyester reçineye ağırlıkça %2 oranında metil-etil-keton-peroksit (MEK-P) sertleştirici olarak ve ağırlıkça %0,2 oranında kobalt reaksiyon hızlandırıcı olarak ilave edilmiştir.

Kompozit içerisinde hava kabarcığı oluşumunu minimum seviyede tutmak amacıyla reçine ağırlığının % 0,5'i oranında, hava uzaklaştırıcı BYK A- 560 kimyasalı kullanılmıştır.

2.2. Yöntem

Alkali İşlem

Kompozitlerin arayüzünü iyileştirmek amacıyla jüt kumaşları kompozit üretiminden önce % 10 oranında sodyum hidroksit (NaOH) çözeltisi ile işleme tabi tutulmuştur [9, 10]. Kumaşların yağ ve kirlerinden arındırılması ve NaOH işleminin efektif olarak yapılabilmesi için jüt kumaşları öncelikle, ağırlıkça %2 noniyonik deterjanla 70°C sıcaklıkta 1 saat süreyle yıkanmıştır. Daha sonra kumaşlar saf su ile durulanıp alkali işleme sokulmuştur.

Alkali işlem için kumaşlar %10 oranında NaOH çözeltisi ile 20°C'de 20 dk işleme tabi tutulmuştur. Daha sonra kumaşlar saf su ile durulanıp, %2 Sülfirik asit (H_2SO_4) çözeltisi ile nötralize edilmiştir. Kumaşlar yeniden saf su ile yıkanmış ve etüvde 70°C sıcaklıkta 8 saat kurutulmuştur. İşlem gören jüt kumaşları kompozit üretimine geçilmezden önce desikatörde 24 saat bekletilmiş ve nem alması engellenmiştir.

Kompozit Üretimi

Jüt kumaşları dikişli ve dikişsiz olmak üzere iki ayrı formda kompozit üretiminde kullanılmıştır. Dikişli kompozitlerde üretimden önce kumaş katları birbirine tip-301 düz dikişle enine ve boyuna 2 cm aralık olacak şekilde dikilmiştir. Dikiş ipliği olarak polyester ipliği kullanılmıştır. Dikişler için ilmik uzunluğu 8 mm olarak seçilmiştir.

Kompozit malzemeler muhtelif lif ağırlık yüzdeleri ile üretilmiştir. Lifin ağırlık yüzdesinin hesaplanmasında aşağıdaki formülasyon takip edilmiştir.

$$\%W_f = \frac{w_f}{w_c} \times 100 \qquad (1)$$

Burada $\%W_f$ kumaşların kütlesel oranı, w_f jüt kumaşların ağırlığı (g), w_c kompozit numunenin ağırlığıdır.

Kompozitler vakum infüzyon tekniği ile üretilmiştir. Şekil 1'de, kullanılan vakum infüzyon düzeneği görülmektedir. İnfüzyon kalıbı olarak 350x350 ebatlarında bir adet demir levha kullanılmıştır. Üretilecek kompozitin yüzeyinin düzgün olması amacıyla demir levha yüzeyi taşlanıp parlatılmıştır. Öncelikle, kalıba numunenin kalıptan kolay ayrılmasının sağlamak amacıyla kalıp ayırıcı sürülmüştür. Daha sonra kalıbın en dış kenarlarına hava sızdırmaz bant yapıştırılmıştır. Vakum torbası bu sızdırmaz bandın üzerine yapıştırılacaktır. Böylece proses sırasında kalıp içine hava girmesi engellenmiş olacaktır. Daha sonra, ön işlemden geçmiş jüt kumaşları kalıbın en iç tarafına yerleştirilmiştir. Lifler yerleştirildikten sonra, oluşacak kompozitin kalıptan kolayca ayrılmasını sağlayan ayırıcı kumaş ve reçine yayıcı kumaş sırasıyla serilmiştir. Yayıcı kumaş üzerine reçinenin daha homojen dağılmasını sağlamak üzere silikon reçine akış kanalları yerleştirilmiş ve ardından vakum torbası en üst katman olarak serilmiştir. İçerideki havanın emilmesiyle vakum torbası, yatırılan malzemenin üzerine bir atmosferlik basınç uygulayarak aşağı çekilir. Böylece reçinenin malzeme tarafından emilmesi sağlanır.

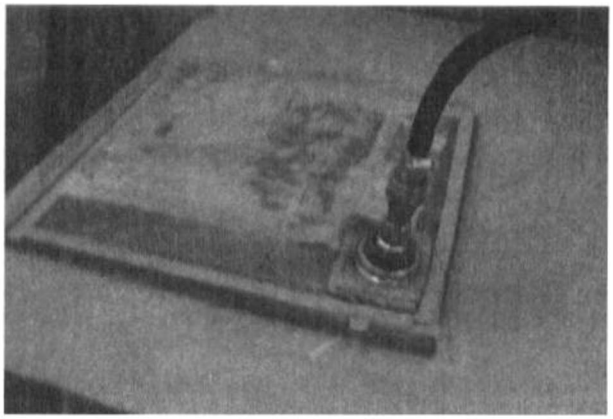

Şekil 1. Vakum infüzyon düzeneği.

Deneysel Tasarım

Kompozitlerin üretim değişkenleri olarak jüt kumaş kat sayısı, alkali işlem ve dikiş durumu (dikişli, dikişsiz) esas alınmıştır.

Değişkenlerin kompozit eğme mukavemetine etkisinin belirlenmesi için bir faktöriyel analiz yürütülmüştür. Faktöriyel analizin yürütülmesinde Minitab® istatistiksel yazılımı kullanılmıştır. Faktöriyel tasarım için kontrol faktörleri Tablo 1'de verilmiştir. 7 farklı üretim varyasyonu ve her varyasyon için 4'lü tekrarlarla toplam 28 adet test yapılmıştır Tablo 2'de kompozitler için deney planı görülmektedir.

Tablo 1. Kompozit mekanik özellikleri faktöriyel tasarımı için kontrol faktörleri.

Faktör	**Seviye**		
	1	**2**	**3**
A: Kat sayısı	2	4	6
B: Dikiş durumu	Dikişli	Dikişsiz	

Tablo 2. Kompozit mekanik test numuneleri için deney planı.

Numune kodu	**Jüt kumaş kat sayısı**	**NaOH işlem kons. (%)**	**Dikiş durumu**	**Ağırlıkça jüt oranı (%)**	**Ağırlıkça PES spacer kumaş oranı**
S1	4	10	Dikişsiz	11,5	1,2
S2	2	10	Dikişsiz	10,7	1,33
S3	6	İşlemsiz	Dikişsiz	29,12	0,87
S4	2	10	Dikişli	10,67	1,36
S5	6	10	Dikişsiz	29,56	0,79
S6	4	10	Dikişli	11,6	1,23
S7	6	10	Dikişli	29,9	0,81

Kompozit Eğme Testi

Kompozitlerin üç noktadan eğme testleri Zwick-Z010 Universal eğme test cihazında ASTM D 790 standardına göre gerçekleştirilmiştir. Eğme testi numuneleri dikdörtgen kesitli plakalar halindedir. Eğme testi için numune boyutları 75x25x4 mm (uzunluk x genişlik x kalınlık) olarak seçilmiştir. Eğici aparat hızı 2,8 mm/dk'dır. Destek span uzunluğu 50 mm'dir. Eğme yüklemesi lif plaka yüzeyine dik olarak (flatwise) gerçekleştirilmiştir (Şekil 2). Her tür kompozit için 4 adet test yapılmış ve ortalama değerler alınmıştır. Testten önce numuneler 23°C sıcaklıkta ve %55 bağıl nemde 40 saat kondisyonlamaya tabi tutulmuştur.

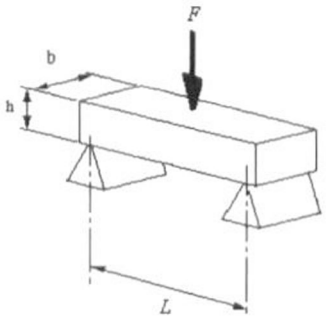

Şekil 2. Üç noktadan eğme testinin görünümü.

Kompozitlerin eğme mukavemeti (σ_b) ve Eğilme elastisite modülü (E_b) sırasıyla şu formüllere göre hesaplanmıştır:

$$\sigma_b = \frac{3FL}{2bh^2} \qquad (2)$$

$$E_b = \frac{mL^3}{4bh^3} \qquad (3)$$

Burada F yük, m yük-çökme eğrisinin başlangıç eğimi, L iki destek arasındaki numune uzunluğu, b numune genişliği, h numune kalınlığıdır.

3. Sonuç ve Yorumlar

Kumaş kat sayısının etkisi

Tablo 3'de numune özellikleri ile birlikte jüt kompozitlerinin eğme testi sonuçları verilmiştir. Numunelerin eğme mukavemeti ve eğme modülü değerleri görülmektedir. Şekil 3 ve Şekil 4'te ise kompozitlerin eğme gerilmesi-çökme grafikleri verilmiştir. Kompozitler yüklemenin başlangıç safhasında tipik lineer karakter sergilemiş daha sonra pseudoplastik bölgeye geçerek maksimum gerilmeye ulaştıktan sonra bir miktar daha uzayarak kopmuşlardır. S6 ve S7 numunelerinde eğilme uzamasının daha fazla

olduğu göze çarpmaktadır. Bu durumun nedeni olarak bu kompozitlerde dikiş ipliklerinin kırılmayı geciktirmek suretiyle uzamayı arttırması söylenebilir.

Kompozit numunelerinde kumaş kat sayısı arttıkça %95 güven aralığı için kompozitlerin eğme mukavemetinin arttığı görülmüştür ($p < 0,05$). Bu durum hem dikişsiz (S1, S2, S5) hem de dikişli (S4, S6, S7) ön şekillerle desteklenen kompozitlerde geçerlidir. Bu durumun nedeni olarak kumaş kat sayısı arttıkça lif ağırlık yüzdesinin artması gösterilebilir. Bilindiği gibi kompozit yapılarda asıl yük taşıyıcı elemen destekleyici liflerdir. Destekleyici liflerdeki artışın mukavemet artışını beraberinde getireceği söylenebilir. İstatistiksel analizler kumaş kat sayısı artışının eğme modülü üzerinde etkili olmadığını göstermiştir ($p > 0,05$).

Tablo 3. Kompozitlerin eğme testi sonuçları

Numune kodu	Jüt kumaş kat sayısı	NaOH işlem kons. (%)	Dikiş durumu	Ağırlıkça jüt oranı (%)	Ağırlıkça PES kor kumaş oranı (%)	Eğme mukavemeti (MPa)	Eğme modülü (MPa)
S1	4	10	Dikişsiz	11,5	1,2	34,17	1016,69
S2	2	10	Dikişsiz	10,7	1,33	29,62	1198,63
S3	6	İşlemsiz	Dikişsiz	29,12	0,87	32,49	1004,00
S4	2	10	Dikişli	10,67	1,36	31,17	1441,97
S5	6	10	Dikişsiz	29,56	0,79	36,68	1145,33
S6	4	10	Dikişli	11,6	1,23	27,11	785,54
S7	6	10	Dikişli	29,9	0,81	36,77	844,94

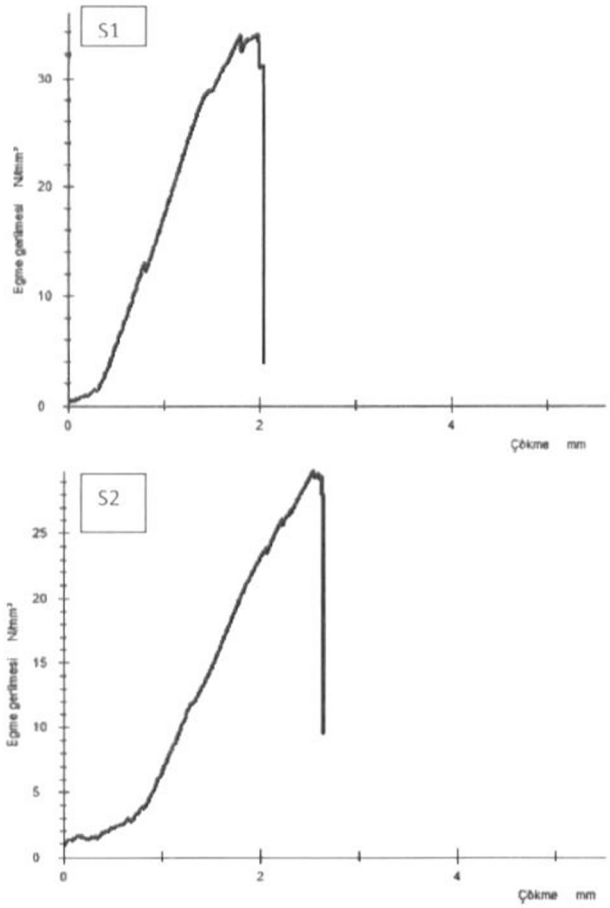
S1
Eğme gerilmesi N/mm²
30
20
10
0
0
2
4
Çökme mm
S2
Eğme gerilmesi N/mm²
25
20
15
10
5
0
0
2
4
Çökme mm

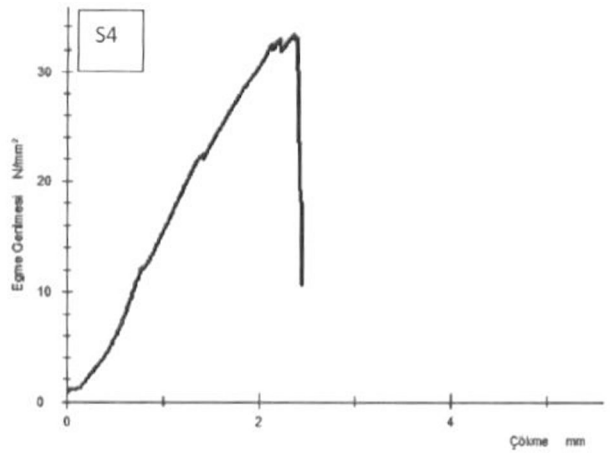

Şekil 3. S1, S2 ve S4 numunelerine ait eğme gerilmesi-çökme grafikleri.

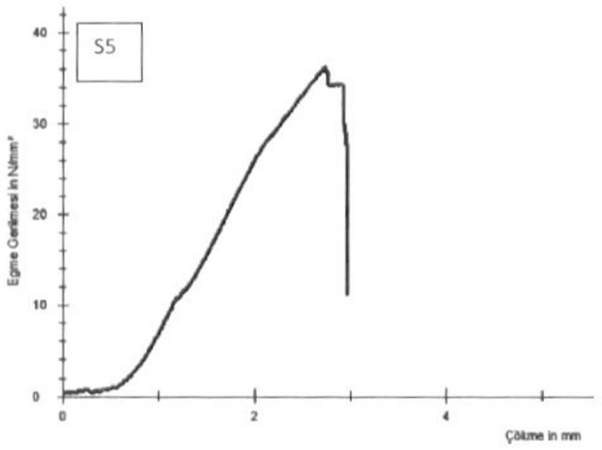

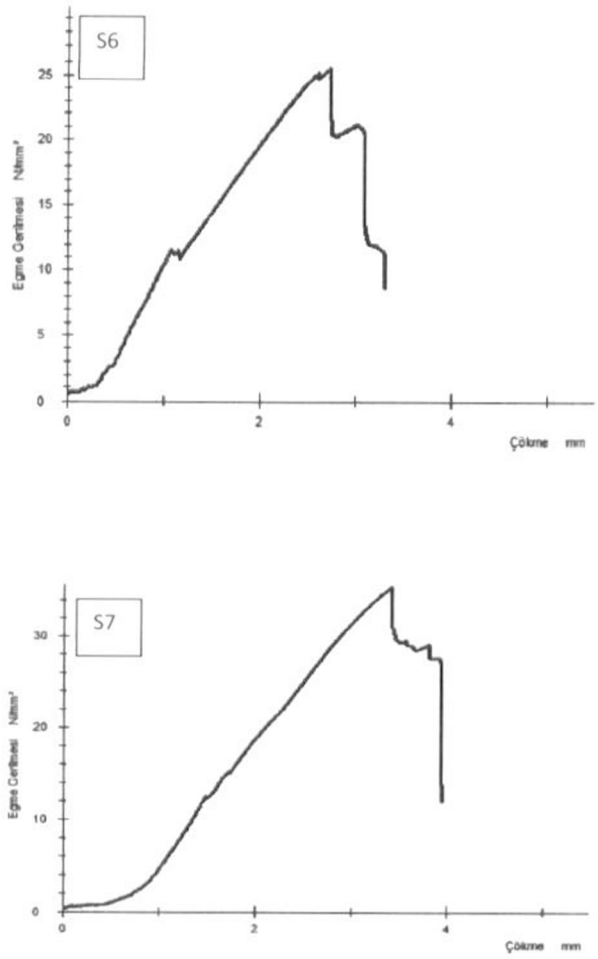

Şekil 4. S5, S6 ve S7 numunelerine ait eğme gerilmesi-çökme grafikleri.

Dikiş durumunun etkisi

Dikişli ve dikişsiz ön şekillerden üretilen kompozitlerin eğme mukavemeti ve eğme modülü değerlerine bakıldığında eğme mukavemeti ve eğme modülünün 2 katlı kumaşla desteklenen numuneler (S2, S4) için dikişle beraber arttığı, bununla birlikte 4 ve 6 katlı kumaşlarla desteklenen numunelerde önemli ölçüde değişmediği veya azaldığı saptanmıştır. Bunun nedeni olarak dikiş işleminin kompozitlerde meydana getirdiği olumlu ve olumsuz etkiler değerlendirilebilir. Dikişin kompozitlerde meydana getirdiği olumlu etki şudur: özellikle tabaka ayrışması (*delaminasyon*) şeklinde oluşan kırılmalarda dikişin katları birbirine tutturarak tabaka ayrışmasını önlediği ve kompozit mekanik özelliklerini geliştirdiği söylenebilir. Fakat bununla birlikte dikişin kompozitler üzerinde şu olumsuz etkilere sahip olduğu gözlemlenmiştir: Dikme işlemi kumaş tabaklarını delmek suretiyle destekleyiciye bir takım hasarlar vermektedir. Bu hasarlar kompozite bir yük bindiğinde özellikle delikli ve yırtıklı bölgelerde gerilme yoğunlaşmaları oluşturarak kompozit mukavemetinin düşmesine yol açmaktadır. Dikiş işleminin bir diğer olumsuz etkisi özellikle 4 ve 6 gibi yüksek kumaş kat sayılarında ön şeklin formunun bozulmasına yol açmasıdır. Özellikle 4 ve 6 katlı kumaş kompozitlerinde (S1, S3, S5, S6, S7) dikişle beraber kumaş formunun bozulduğu ve buna bağlı olarak üretilen kompozit plakalarda ince-kalın yerlerin oluştuğu gözlemlenmiştir. İnce-kalın yerler kompozitlerde yük dağılım dengesini bozarak ve lokal gerilme yığılmaları (*stress concentration*) oluşturarak nihai kompozit mukavemetini düşürmektedir. Buna karşın 2 katlı kumaşlar nispeten daha ince olduğu için dikişle bu kompozitlerde meydana gelen ince-kalın yer varyasyonları görece daha az olmaktadır. Bu durum 4 ve 6 katlı kompozitlerde dikişle beraber mukavemet ve modülün düşmesini getirirken, 2 katlı kumaş kompozitinde dikişle birlikte mukavemetin ve modül değerinin artmasını sağlamıştır.

NaOH işleminin etkisi

NaOH işlemli ve işlemsiz kumaşlarla desteklenen kompozitlerin (S5, S3) mekanik değerlerine bakıldığında NaOH işlemiyle birlikte eğme mukavemeti ve modülünün arttığı görülmektedir (Tablo 3). Eğme özelliklerindeki bu artışa sebep olarak NaOH işlemiyle birlikte lif-reçine arayüzünün iyileşmesi, dolayısıyla lif ve reçinenin birbirine daha iyi entegre olması gösterilebilir. Alkali işlem sonucunda liflerde oluşan fibriler yapı sebebiyle lifin reçine ile çok daha iyi ıslandığı ve birleştiği söylenebilir.

4. Sonuç

Doğal lif takviyeli polimerik kompozitlerin önemi gün geçtikçe artmaktadır. Bu çalışmada vakum infüzyon tekniğiyle üretilen sandviç yapılı jüt kumaşı/polyester gözenekli kumaş destekli kompozitlerin eğilme özellikleri araştırılmıştır. Bu kapsamda kumaş kat sayısı, dikiş durumu ve NaOH işlemi gibi faktörlerin kompozitlerin eğilme özelliklerine etkisi gözlemlenmiştir.

Kompozit numunelerinde kumaş kat sayısı arttıkça eğme mukavemetinin arttığı görülmüştür. Bu durumun nedeni olarak kumaş kat sayısı arttıkça lif ağırlık yüzdesinin artması gösterilmiştir.

Eğme mukavemeti ve eğme modülünün 2 katlı kumaşla desteklenen numuneler için dikişle beraber arttığı, bununla birlikte 4 ve 6 katlı kumaşlarla desteklenen numunelerde önemli ölçüde değişmediği veya azaldığı saptanmıştır. Bunun nedeni olarak 2 katlı kumaşların nispeten ince olduğu için dikişle bu kompozitlerde meydana gelen ince-kalın yer varyasyonlarının 4 ve 6 katlı kompozitlere göre daha az olması gösterilmiştir.

NaOH işlemiyle birlikte kompozitlerin eğme mukavemeti ve modülünün arttığı görülmüştür. Bu artışa sebep olarak NaOH işlemiyle birlikte lif-reçine arayüzünün iyileşmesi gösterilmiştir.

Çalışma sonucunda jüt kumaşı takviyeli sandviç yapılı kompozitlerin otomotiv ve yat endüstrileri gibi hafif yapısal malzemelerin önemli olduğu alanlarda kullanılabileceği öngörülmüştür.

5. Kaynaklar

1. Bledzki AK, Faruk O, Sperber VE. Cars from bio-fibres. Macromol. Mater. Eng 2006;(291):449–457.
2. Böttcher P, Vliessitoffe Tech. Text. 2002,2,35.
3. Kaup M, Karus M. Naturfasern für die Europaische automobilindustrie, 2002 Nova Institute, http://www.nova-institut.de.
4. Fung F, Hardcastle M. Textiles in automotive engineering. Woodhead Publishing Ltd. Cambridge, England 2001.
5. Suddel BC, Evans WJ. Natural fiber composites in automotive applications, In: Natural Fibre Biopolymers and Biocomposites. Mohanty AK, Misra M, Drzal LT. CRC Press, USA 2005.
6. Rana, A. K., Jayachandran, K., Jute Fibers for Reinforced Composites and Its Prospects, Molecular Crystals and Liquid Crystals, 353, 35-45, 2000.

7. Parikh, D.V., Chen, Y., Sun L., Reducing Automotive Interior Noise with Natural Fiber Nonwoven Floor Covering Systems, Textile Research Journal, 76, 813-820, 2006.
8. Gassan, J., Bledzki, A. K., Thermal Degradation of Flax and Jute Fibers, Journal of Applied Polymer Science, 82, 1417-1422, 2001.
9. Onal, L. and Karaduman Y. (2009). Mechanical Characterization of Carpet Waste Natural Fiber Reinforced Polymer Composites, *Journal of Composite Materials*, **43**(16):1751-1768.
10. Onal L, Goktepe F, Karaduman Y. Characterisation of jute carpet waste for natural fibre reinforced composite production, 7th Global WPC and Natural Fibre Composites Congress and Exhibition, Kassel, Germany 2008. p. B18-1 – B18-8.

FABRICATION OF MULTIFUNCTIONAL CARBON NANOTUBE – POLYMER COMPOSITES BY SOPHISTICATED PROCESSING TECHNIQUES

Dimitrios Tasis

Department of Materials Science, University of Patras, 26504 Patras, GREECE
Email address: dtassis@upatras.gr

Abstract
The properties and applications of carbon nanotubes (CNTs) and related materials has been a very active research field over the last decade. It is indeed the combination of their exotic properties that makes them the ideal filler in a number of composite applications. During the last years, there have been many studies dedicated to processing and fabrication of multifunctional polymer nanocomposites. Yet, several obstacles have been found to hamper dramatically the preparation of homogeneous CNT-based polymer composites. So far, the majority of the processing methods leads to materials that contain low volume fractions of CNTs that, at least in absolute mechanical property values, cannot seriously compete with commercial polymer composites. Yet, in some recent studies, the superb properties of CNTs have been shown to be fully translated into high strength and stiffness of finished products.

1. Introduction

A nanocomposite is defined as a composite material where at least one of the dimensions of one of its components is on the nm size scale. The challenge and interest in developing nanocomposites is to find ways to create functional materials that benefit from the unique physicochemical properties of nano-sized structures within them. Natural materials such as bone, teeth etc are very good examples of successful incorporation of inorganic nanostructures within various organic matrices [1]. Such composites exhibit perfectly organized levels of hierarchical structure, offering excellent mechanical enhancement compared to the constituent components. The idea of creating multifunctional composite materials with improved performance using a wide variety of matrices is currently under development, although the focus has been mainly given to polymeric systems. Similarly, the filler particles can be organic or inorganic with a wide range of compositions and sizes. Carbon nanotubes (CNTs) have attracted great interest among the researchers due to their exotic physical and structural properties. The combination of these properties suggests that CNTs can act as potential fillers in high-performance polymer composites. During the last decade or so, there has been tremendous progress in the scientific area of CNT/polymer composites which enabled potential advancements in various sectors

of nanotechnology, ranging from ultrastrong materials for bullet-proof vests to flexible displays and sports equipment [2]. With CNTs becoming easier to produce and cheaper to buy, the CNT industry could potentially overtake that of the carbon fiber industry and become one of the major additives for polymer composite fabrication.

In this survey, the development of functional CNT/polymer composites during the recent years will be addressed in detail. The focus will be on the processing methods for fabricating super-strong and/or conductive composite materials.

2. Processing methods

Many research efforts have been directed towards producing CNT/polymer composites for functional and structural applications. However, even after a decade of research, the full potential of employing CNTs as reinforcements has been severely limited due to difficulties associated with dispersion of entangled CNTs during processing and poor interfacial interaction between CNTs and polymer matrix. The nature of dispersion problem for CNTs is rather different from other conventional fillers, such as spherical particles and carbon fibers, because CNTs have high aspect ratio (>1000) and thus extremely large surface area. In addition, the commercialized CNTs are supplied in the form of heavily entangled bundles, resulting in inherent difficulties in dispersion.

In order to maximize the potential of CNTs as effective filler in polymer composites, the graphitic nanostructures should be homogeneously dispersed within the matrix. Common processing methods for the fabrication of CNT/polymer composites include solution mixing, in situ polymerization, melt mixing and melt spinning. These methods have been comprehensively discussed in recent review articles [3-6], therefore, we are going to present an overview of the most important accomplishments. In addition, some recent non-traditional processing techniques will be documented. All the aforementioned methods try to address issues that affect the composite properties, such as exfoliation of CNT bundles, homogeneous dispersion of individual tubes in the matrix, CNT alignment and interfacial interaction between the filler and the matrix.

2.1 Common approaches

The method of solution mixing/casting is one of the most used approaches for preparing CNT/ polymer composites in a lab scale [7-10]. The nanotubes and polymer are mixed in a suitable medium, followed by evaporation of the solvent to result in a composite film. Generally, dispersion of the nanotubes is done separately from dissolution of the polymer because the high shear processes typically involved in dispersion would likely cause molecular weight degradation of the polymer. During the first stage of a typical protocol, the most efficient method for the dispersion of CNT materials in a specific solvent can be achieved by bath or tip ultrasonication. This involves the application of ultrasound energy for the agitation

of particles in a solution. It is the most frequently used method for nanoparticle dispersion. The principle of this technique is that when ultrasound propagates in a liquid solvent, attenuated waves are induced in the molecules of the medium through which it passes. The production of these shock waves promotes the ''peeling off'' of individual nanoparticles located at the outer part of the nanoparticle bundles and thus results in their partial or full exfoliation.

In addition, chemical functionalization of the CNT sidewalls and tips has been used to assist dispersion and enhance the chemical affinity with the polymer matrix [11-14]. For the last step (solvent evaporation), the casting technique has been mainly utilized. Since the casting/evaporation process is a relatively slow procedure resulting in the re-agglomeration of the carbon nanostructures within the composite, researchers have alternatively used the spin coating technique in order to succeed rapid evaporation of the solvent medium [15,16]. In their seminal work, Safadi et al. [15] have elucidated the basic relationships between simple casting and spin casting conditions, concluding that the processing method employed had no effect on the mechanical/electrical properties of the CNT-based composite.

In a very interesting work, Winey and co-workers [17] have established the coagulation method, in which a CNT/polymer stable suspension was poured dropwise into a large excess of bad solvent, resulting in the instantaneous precipitation of the polymer chains and the trapping of the isolated carbon nanostructures. After isolation of the final composite, it was concluded that CNTs were homogeneously distributed in the thermoplastic matrix (PMMA).

One of the advantages of the 'solution mixing' method is the possibility to achieve debundling and good-quality dispersion of the CNT material in an appropriate medium. However, solution processing techniques cannot be utilized for insoluble polymers. One additional problem with the solution mixing method is the fact that no environmentally-friendly medium exists that is able to both dissolve most polymers and disperse CNT material efficiently. One recent development is the use of supercritical fluids to assist in this process. Evaporation can be very quick by simply releasing the pressure. Using a mixture of acrylic monomer and supercritical carbon dioxide, interesting microstructures of various polymers on CNTs have been produced [18].

Using alternative approaches, researchers have used the roll-casting technique [19]. The roll-cast system comprises two opposing parallel rollers with a gap distance that can be adjusted. A suspension of a CNT/polymer mixture can be slowly dropped onto one roller when rotating, while a solid film is formed after evaporation of the solvent. In an analogous strategy, the groups of Schulte [20] and Chou [21] studied the dispersion of CNTs into viscous epoxy monomers via a common shear mixing technique, that is, calendering. The calender, or commonly known as three roll mills, is a machine tool that employs the shear force created by rollers to mix, disperse or homogenize viscous materials. The general configuration of a calendering machine consists of three adjacent cylindrical rollers each of which runs at a different velocity. The first and third rollers, called the feeding and apron roller rotate in the same direction while the center roller rotates in the opposite direction. The material

to be mixed is fed into the hopper, where it is drawn between the feed and center rollers. When pre-dispersed, the material sticks to the bottom of the center roller, which transports it into the second gap. In this gap, the material that remains on the center roller is subjected to even higher shear force due to the higher speed of the apron roller. This milling cycle can be repeated several times to maximize dispersion. The narrow gaps (mechanically or hydraulically adjusted from 500 to about 5 μm) between the rollers, combined with the mismatch in angular velocity of the adjacent rollers, result in locally high shear forces with a short residence time. By using this processing method, formation of a conductive percolating network at CNT concentrations below 0.1% by weight was enabled in the as-prepared polymer composites. The thermal conductivity increased linearly with nanotube concentration to a maximum increase of 60% at 5 wt.% CNTs [20,21].

When dealing with thermoplastic matrices, which are insoluble in aqueous or organic media, melt processing is the preferable technique for fabricating CNT-based composites [22-24]. The major advantage of this method is that no solvent is employed to disperse CNTs. In addition, melt mixing is the most promising approach for the fabrication of CNT/polymer composites in industrial scale. In general, melt processing involves the mixing of polymer melt with CNTs by application of intense shear forces. Depending on the final morphology/shape of the composites, the bulk samples can then be processed by several techniques, such as extrusion, injection molding and compression molding [25].

Except the case of bulk composites, melt processing can also be utilized for the fabrication of composite fibers, through the melt spinning/drawing technique [22, 26]. Melt spinning is the preferred method of manufacture for polymeric fibers. The polymer is melted and pumped through a spinneret (die) with numerous holes (one to thousands). The molten fibers are cooled, solidified, and collected on a take-up wheel. Stretching of the fibers in both the molten and solid states provides for orientation of the polymer chains along the fiber axis. Polymers such as poly(ethylene terephthalate) and nylon 6,6 are melt spun in high volumes. One of the main drawbacks of the melt processing method is considered the potential of thermal degradation and/or oxidation of the polymeric matrix during the heating period.

As a versatile alternative approach, in situ polymerization of vinyl monomers in the presence of CNTs has been extensively studied during the last decade [27-30]. The main advantage of this method is that it produces chemically modified tubes with grafted polymer chains, mixed with free polymer chains. Moreover, due to the small size of monomers, the homogeneity of the resulting composite adducts is much higher than mixing CNTs and long polymer chains in solution. In this sense, the method allows the preparation of composites with high CNT weight fraction.

Concerning the preparation of anisotropic CNT–polymer composites by in situ polymerization process, Kimura et al. [31] have mixed styrene monomer with nanotubes and subjected the suspension to a constant magnetic field of 10 T. By polymerizing the mixture, the nanotubes were found to be kept aligned within the polymer matrix. Analogous experiments with an epoxy thermoset as a matrix showed that the thermal and electrical properties of the composites were

significantly enhanced by magnetic alignment during processing [32]. In an analogous work, Bauhofer and co-workers [33] dispersed MWCNTs in an epoxy system based on a bisphenol-A resin and an amine curing agent. The application of both AC and DC electric fields during nanocomposite curing was used to induce the formation of aligned conductive nanotube networks between the electrodes. The network structure formed in AC fields was found to be more uniform and more aligned compared to that in DC fields.

2.2 Novel approaches

2.2.1 CNT-based membranes and networks

A very versatile approach, the layer-by-layer (LBL) approach involves building up a composite film by alternate dipping of a glass substrate into a dispersion of CNTs and a polymer solution. This protocol results in the adsorption of CNT and polymer monolayers onto the glass surface and the formation of a composite film with thickness in the μm scale [34,35]. In order to improve the structural integrity of the film, chemical crosslinking can be induced by heating at 120 ^{0}C and/or using bifunctional reagents, such as glutaraldehyde [36]. This approach provides multifunctional composites with layered structure. This method has significant advantages as thickness and nanotube/polymer ratio can easily be controlled and very-high nanotube loading levels can be obtained (about 50 wt%). The only drawback is that it is a relatively slow process. Such LBL-assembled composites have shown potential applications, such as transparent and flexible conductors [37], sensors [38], and neural interface electrodes [39].

In order to prepare CNT/polymer composites with a high CNT loading, independent groups have studied the impregnation of organic thermosetting prepolymers [40] and polymers [41] into the porous macroscopic sheets of randomly entangled CNTs, called buckypapers. The latter can be prepared by filtration of either surfactant-stabilized CNT suspensions or oxidized CNT material in water [42]. The thickness of these CNT preforms ranges between 50 and 200 μm, whereas the porosity is about 75%. The intercalation process could be obtained by simply soaking the nanotube sheets in polymer [41] or epoxy-based prepolymer solutions [40]. The resulting polymer-intercalated sheets displayed improvements in Young's modulus and tensile strength, compared to pristine CNT sheets as well as the neat matrix. A similar impregnation technique was demonstrated by Wang and co-workers [43]. They also prepared buckypapers, but impregnated an epoxy-hardener blend into their free pores by a filtration process along the thickness direction. To reduce the viscosity, the blend was slightly diluted with acetone (ratio of epoxy prepolymer to acetone about 70:30). A hot press molding process was used for curing the final nanocomposites having high CNT loading (up to 40 wt%). The research results showed that the proposed buckypaper/resin infiltration approach is quite suitable for the fabrication of nanocomposites with controllable nanostructure and high CNT

loading, which are important for the development of high performance nanotube-based composites.

In all the aforementioned cases, the orientation of the carbon nanostructures within the composites is random.

To maximize the translation of individual nanotube mechanical and physical properties to the macroscopic film level, it is attractive to align the CNTs in one in-plane direction. The groups of Colbert and Wang, independently, reported the fabrication of such CNT sheets, which were produced by filtrating single-walled CNT suspensions in a 17.3T magnetic field [42, 44]. In addition, they studied the electrical, thermal and mechanical properties of the neat buckypapers as well as of their polymer composites. In the nanocomposites, the CNT volume loading was about 50% for aligned composites and 25–30% for random composites. It has to be stated that the magnetic alignment method can not be widely applied since the high magnetic field makes the broad application of this process inconvenient and the problems of nanotube waviness and agglomeration are not easily resolved.

In an alternative approach, Liang and co-workers [45] fabricated CNT-sheet-reinforced bismaleimide (BMI) resin nanocomposites with high concentrations (60 wt%) of aligned tubes. Applying simple mechanical stretching and prepregging (pre-resin impregnation) processes on commercially available sheets of randomly dispersed millimeter-long MWCNTs lead to substantial alignment enhancement of the carbon nanostructures as well as high packing density of nanotubes in the resultant nanocomposites. In the first stage, the authors used a simple mechanical-stretch method to align the carbon nanostructuress in the buckypaper sheets. For example, for a 40%- stretched CNT sheet (i.e., the post-stretch sheet was 40% longer than the pre-stretch sheet), the degree of alignment of the CNT sheet was shown to be dramatically improved.

Load carrying along the alignment direction showed improvements from the post-stretching samples. The mechanical properties of the neat MWCNT sheets of different stretch ratios were measured. The tensile strength at break and Young's modulus of a randomly dispersed CNT sheet (the control sample) were approximately 205 MPa and 1.10 GPa, respectively. During stretching, the MWCNTs self-assembled and aligned themselves along the load direction. The MWCNT rope sizes increased and the packing density became higher compared to pre-stretched MWCNT sheets. Along the alignment direction, the mechanical properties were significantly improved. The tensile strengths increased to 390, 508 and 668 MPa for the 30%, 35%, and 40% stretched samples, corresponding to 90%, 148% and 226% improvements, respectively. The post-stretch Young's modulus measurements along the alignment direction showed even more dramatic improvements, from 1.10 GPa for the randomly dispersed sheet (pre-stretch) to 11.93, 18.21 and 25.45 GPa, respectively. In a subsequent step, the CNT dry perform was impregnated into a BMI resin solution in acetone, under pressure conditions. Curing of the resulting prepreg resulted in superstrong as well as conductive composite films.

Concerning the mechanical properties of the composites, the tensile strength of the randomly dispersed MWCNT/BMI composite (the control sample) was approximately 620 MPa and the Young's modulus was 47 GPa. After stretching to improve alignment and nanotube packing, the tensile strength and Young's modulus of the 30%-stretched CNT/BMI composite were 1600 MPa and 122 GPa, respectively. When the stretch ratio increased to 35%, the tensile strength and Young's modulus increased respectively to 1800 MPa and 150 GPa. The tensile strength and Young's modulus of the 40%-stretched MWCNT/BMI composite were as high as 2088 MPa and 169 GPa, respectively.

Unprecedentedly high electrical conductivity was also realized in the stretched-MWCNT/BMI composites. The electrical conductivity along the alignment direction of the CNTs was significantly higher than that of pre-stretched control samples (915 S cm^{-1}). An increasing degree of alignment raised the electrical conductivity: 1800 S cm^{-1} for the 30%-stretched specimen, to 3000 S cm^{-1} for the 35%-stretched specimen, and 5500 S cm^{-1} for the 40%-stretched specimen. These high conductivity measurements were attributed to: i) high concentrations of MWCNTs in the composite samples (60 wt%), ii) millimeter-long MWCNTs without functionalization that preserved intrinsic electrical conductivity, and iii) dense packing of MWCNTs leading to better contacts among nanotubes.

Recently, the same group reported that chemical functionalization of the CNT sheets by epoxidation reaction - prior to impregnation step - improved further the mechanical properties of the CNT/resin composite membranes [46]. The tensile strength and Young's modulus of functionalized random CNT-sheet/BMI nanocomposites reached 1437 MPa and 124 GPa, respectively, which are about two times greater than those of pristine random CNT-sheet/BMI nanocomposites previously reported [45]. For functionalized 40%-stretch aligned CNT-sheet/BMI nanocomposites, the tensile strength and Young's modulus reached 3081 MPa and 350 GPa, respectively. These values are 48 and 107% higher over those of pristine 40%-stretch CNT-sheet/BMI nanocomposites. Such CNT-based polymer composites have exhibited the highest values of tensile strength and elastic modulus, among the reported data of literature.

Alternatively, for producing buckypapers with long and aligned CNTs, independent groups [47,48] developed a sophisticated method, called the 'domino pushing process' starting with a carpet of aligned arrays of CNTs (forest). The aligned multi-walled CNT arrays were fabricated by a chemical vapour deposition (CVD) method. All CNTs in the aligned CNT arrays are considered to be long and extend from the bottom to the top, forming a thick CNT forest standing on the silicon substrate. The 'domino pushing' method comprises the following three steps:

(a) The CNT array is covered with a piece of microporous membrane and all the CNTs of the CNT array are forced down to one direction by pushing a cylinder which is placed upon the CNT array with constant pressure. Thus, all CNTs in the CNT array form an aligned buckypaper.

(b) The aligned buckypaper is peeled off from the silicon substrate with the membrane, and

(c) Liquid solvent is spread on the microporous membrane so the aligned buckypaper can be peeled off from the membrane easily.

These aligned CNT buckypapers with controllable structure exhibit many potential applications, such as supercapacitor electrodes [47] as well as dry preforms for polymer impregnation [48]. Due to the alignment of the carbon nanostructures, the 'domino pushing' approach has shown great potential in producing CNT composites with strength and stiffness superior to current commercial composites.

By using a sophisticated spinning process, Fan and co-workers [49] developed a method to form continuous CNT sheets by directly drawing CNTs from super-aligned CNT arrays. In this manner, the carbon nanostructures can be joined end to end by van der Waals interactions to form a continuous and aligned CNT sheet. Many of these continuous and aligned CNT sheets can be stacked together to make a CNT preform with thickness on a centimeter scale. In a subsequent study of the same group, such CNT preforms have been used as structural reinforcements for fabricating CNT/epoxy composite films by Vacuum-Assisted Resin Infiltration (VARI) method [50]. Composite films with CNT weight fraction ~8% exhibited Young's modulus value of about 11 GPa (347% improvement), whereas the corresponding value for tensile strength was about 130 MPa (50% enhancement). Analogous experiments have been recently performed by using Resin Transfer Molding (RTM) technique [51]. RTM involves placing a textile preform into a mold, injecting the mold with a liquid resin at low injection pressure, and curing the resin to form a solid composite. RTM is a simple process that can make composites with large sizes and complex shapes within short cycle time and at low cost and can be applied to many kinds of low-viscosity thermosetting polymers. These CNT/epoxy composites showed significantly improved mechanical and electrical properties with Young's modulus up to 20.4 GPa, tensile strength up to 231.5 MPa, and electrical conductivity up to 13000 S/m.

A controlled, efficient and cost-effective method to produce CNT/polymer composites, in which the density and position of the tubes within the composite can be controlled, was developed by independent groups. In the first step, CNTs were grown by chemical vapor deposition on pre-patterned templates in the form of either aligned dense arrays (forests) [52,53], periodic arrays [54] or sponges [55]. These CNT networks were then incorporated into a polymer matrix by spin coating a curable prepolymer film on the as-grown tubes. Such polymer composites showed electrical resistivity comparable to pure CNT scaffolds. This controlled method of producing free-standing nanotube/polymer composite films represents an efficient method of combining these materials for potential flexible electronic applications in an inexpensive and scalable manner. In an analogous processing strategy, Valentini et al. [56] used electrodeposited CNTs as templates for the preparation of semi-transparent conductive films by infiltration of methyl methacrylate and subsequent polymerization into the free pores of the CNT film.

2.2.2 CNT-based fibers

In a different approach for preparing CNT/polymer composites, researchers have focused their efforts in the fabrication of composite micro- or nano-fibers. Fiber production techniques are best suited for obtaining aligned tubes within the polymer matrix, thus providing super-strong composite materials.

Apart from the traditional melt spinning method discussed above, composite fibers can also be produced by solution-based processing, such as the coagulation-spinning method. In the work of Vigolo et al. [57], SWCNTs were dispersed homogeneously in a surfactant solution. Nanotube aggregation was obtained by injecting the CNT dispersion into a rotating aqueous bath of PVA, such that nanotube and PVA dispersions flowed in the same direction at the point of injection. Due to the tendency of the polymer chains to replace surfactant molecules on the graphitic surface, the nanotube dispersion was destabilized and collapsed to form a fiber. These wet fibers could then be retrieved from the bath, rinsed and dried. Significant rinsing was used to remove both surfactant and PVA. Shear forces during the flow lead to nanotube alignment. These fibers displayed tensile moduli and strength of 9–15 GPa and ~150 MPa, respectively.

Two years later, the same group developed a modified protocol in order to enhance further the tensile behaviour of the CNT fibers containing small amounts of polymer [58]. The authors observed that the mechanical properties of these fibers could be significantly improved by stretching when wet. This tended to align the nanotubes further, resulting in moduli of ~40 GPa and strengths of up to 220 MPa. Using solvents that possess lower chemical affinity with the polymer appeared to yield better SWNTs alignments. The authors hypothesized that in a poorer solvent there are less sliding effects and that the cohesion of the nanotubes–polymer network is better within the fibrilar structure.

Utilization of denaturated single-stranded DNA as a surfactant for the preparation of the CNT dispersion gave poorer mechanical results. For stretched CNT/DNA/PVA fibers, the tensile moduli and strength were ~19 GPa and ~125 MPa, respectively [59]. In the meantime, the coagulation-spinning method was further optimized by Baughman and co-workers [60]. They injected the SWCNT dispersion into the center of a coflowing PVA/water stream in a closed pipe. The wet fiber was then allowed to flow through the pipe before being wound on a rotating mandrel. Flow in more controllable and more uniform conditions in the pipe resulted in more stable fibers. Crucially, wet fibers were not rinsed to remove most of PVA (final SWCNT weight fraction ~60%). This resulted in large increases in Young's modulus and strength to 80 and 1.8 GPa, respectively.

By adopting the protocol of Vigolo et al. [57], Poulin and co-workers [61] used a hot-drawing treatment, a concept inspired from textile technologies, to improve the properties of CNT/PVA fibers. The authors have shown that single- and multi-walled CNT-based fibers (containing equal amount of CNTs and PVA polymer) could be drawn at temperatures above the PVA glass transition temperature (~180

^{0}C), resulting in improved nanotube alignment and polymer crystallinity. The latter has been shown to be critical to enhancing stress transfer between nanotubes and polymer in composite materials. These so-called hot-stretched fibers exhibited values of elastic moduli between 35 and 45 GPa and tensile strengths between 1.4 and 1.8 GPa, respectively. The higher strain-to-failure value was estimated about 11%, whereas the toughness was about 55 J/g, which is significantly higher than the toughness of Kevlar.

A sophisticated method for obtaining high strength polymer fibers is gel spinning. Some high-strength polyethylene and aramid fibers are produced by gel spinning. The technique depends on isolating individual chain macromolecules in the solvent so that intermolecular entanglements are minimal. Entanglements make chain orientation more difficult, and lower the strength of the final product. Not completely separated, as they would be in a true solution, the polymer chains are bound together at various points in liquid crystal form. This produces strong inter-chain forces in the resulting filaments that can significantly increase the tensile strength of the fibers. In their seminal studies, the groups of Kumar [62] and Wang [63] studied independently the fabrication of CNT/polymer fibers by gel spinning technique. The CNT/polymer blend was not in a true liquid state. In the form of a precisely-heated gel is processed by an extruder through a spinneret. The extrudate was drawn through the air and then cooled in a bath of bad solvent. The end-result is a fiber with a high degree of molecular orientation, and therefore exceptional tensile strength. In addition, the liquid crystals are aligned along the fiber axis by the shear forces during extrusion. The modulus and the tensile strength of the PVA/CNT (3 wt%) composite fiber was 40 and 20% higher than that of the control PVA gel spun fiber, respectively [62].

Using a similar protocol, CNT/polymer solutions have been spun into fibers using a dry-jet wet spinning technique [64-66]. This was achieved by extruding a hot CNT/polymer solution through a cylindrical die. The extrusion jet was placed a small distance above the coagulation bath, which is maintained at room temperature. The nascent fibers descend into the liquid, pass under a guide and proceed in the bath while undergoing stretch. Then, they are withdrawn from the bath and wound up. Significant mechanical property increases were recorded for the composite fibers compared with the control samples with no CNT reinforcement. The tensile modulus and tensile strength of the CNT/polyacrylonitrile composite fiber (10% CNT weight fraction) were higher than the values for the neat polymer fiber by approximately 100 and 45%, respectively [66].

Another method used recently to form composite-based fibers from solution is electrospinning. This technique involves electrostatically driving a jet of polymer solution out of a nozzle onto a metallic counter-electrode. In 2003, two groups independently described electrospinning as a method to fabricate CNT–polymer composite fibers [67,68]. Composite dispersions of CNTs in either PAN or PEO in DMF and ethanol/water, respectively, were initially produced. Electrospinning was carried out using air pressure of 0.1–0.3 kg/cm^2 to force the solution out of a syringe 0.5 mm in diameter at a voltage difference of 15–25 kV with respect to the collector.

Charging the solvent caused rapid evaporation resulting in the coalescence of the composite into a fiber which could be collected from the steel plate. Fibers with diameters between 10 nm and 1 μm could be produced in this fashion.

In an alternative approach, CNT fibers were prepared by the 'direct spinning' method from a CVD reaction zone [69]. Such CNT fibers exhibited diameters of about 10 μm and density values between 0.3 and 1.1 g/cm^3. The tensile strength of the resulting CNT fibers was estimated about 9 GPa [70]. Such aligned fibers of CNTs have been impregnated with epoxy [71] in order to improve the load-bearing capability of CNTs inside fibers. In the work of Windle and co-workers [71], CNT fibers having tensile strength ~0.55 GPa and modulus ~22 GPa were infiltrated with an epoxy monomer/curing agent mixture within a special mould. Tensile and compression tests showed that the composite stiffness and fiber volume fraction are fully related parameters. Moreover, on the assumption that the specimens are unidirectional composites, the ultimate tensile strength of CNT-fiber composites was found to be 90% of the value predicted by the simple rule of mixtures. Composites with CNT volume fraction of about 27% exhibited stiffness and tensile strength values 18.8 GPa and 253 MPa, respectively.

In a similar approach, Xie and co-workers [72] have synthesized CNT films by CVD method. The reticulate architecture of the nanotube bundles showed enhanced potential for fabricating super-strong polymer composites, due to its advantage on evenly delivering load over a large interfacial area. In a recent study, the same group fabricated composite fibers with enhanced tensile strength and modulus [73]. The CVD-grown CNT films were firstly split into narrow strips. After the intercalation of either epoxy prepolymer or PVA by solution infiltration process, they were fabricated into fibers through a twisting process. Finally, the polymer-intercalated fibers were cured or dehydrated in an oven at elevated temperature. The strength values for epoxy- and PVA-infiltrated fibers ranged from 0.9 to 1.6 GPa and 0.7 to 1.3 GPa, respectively. Concerning the elastic modulus values for the epoxy- and PVA-infiltrated fibers, these ranged from 30 to 50 GPa and 20 to 35 GPa, respectively.

References

[1] R. Zapanta LeGeros, *Chem. Rev.* **2008**, *108*, 4742.
[2] O. Breuer, U. Sundararaj, *Pol. Compos.* **2004**, *25*, 630.
[3] B. P. Grady, *Macromol.Rapid Commun.* **2010**, *31*, 247.
[4] M. T. Byrne, Y. K. Gunko, *Adv. Mater.* **2010**, *22*, 1672.
[5] T.-W. Chou, L. Gao, E. T. Thostenson, Z. Zhang, J.-H. Byun, *Compos. Sci. Technol.* **2010**, *70*, 1.
[6] Z. Spitalsky, D. Tasis, K. Papagelis, C. Galiotis, *Progr. Pol. Sci.* **2010**, *35*, 357.
[7] P. M. Ajayan, O. Stephan, C. Colliex, D. Trauth, *Science* **1994**, *265*, 1212.
[8] L. Jin, C. Bower, O. Zhou, *Appl. Phys. Lett.* **1998**, *73*, 1197.
[9] M. S. P. Shaffer, A. H. Windle, *Adv. Mater.* **1999**, *11*, 937.
[10] L. Qu, Y. Lin, D. E. Hill, B. Zhou, W. Wang, X. Sun, A. Kitaygorodskiy, M. Suarez, J. W. Connell, L. F. Allard, Y.-P. Sun, *Macromolecules* **2004**, *37*, 6055.

[11] D. E. Hill, Y. Lin, A. M. Rao, L. F. Allard, Y.-P. Sun, *Macromolecules* **2002**, *35*, 9466.
[12] C.-H. Tseng, C.-C. Wang, C.-Y. Chen, *Chem. Mater.* **2007**, *19*, 308.
[13] T. Chatterjee, C. A. Mitchell, R. A. Hadjiev, V. G. Krishnamoorti, *Adv. Mater.* **2007**, *19*, 3850.
[14] T. J. Simmons, J. Bult, D. P. Hashim, R. J. Linhardt, P. M. Ajayan, *ACS Nano* **2009**, *3*, 865.
[15] B. Safadi, R. Andrews, E. A. Grulke, *J. Appl. Pol. Sci.* **2002**, *84*, 2660.
[16] R. H. Schmidt, I. A. Kinloch, A. N. Burgess, A. H. Windle, *Langmuir* **2007**, *23*, 5707.
[17] F. Du, J. E. Fischer, K. I. Winey, *J. Pol. Sci. B* **2003**, *41*, 3333.
[18] B. Yue, Y. Wang, C. Y. Huang, R. Pfeffer, Z. Iqbal, *J. Nanosci. Nanotechnol.* **2007**, *7*, 994.
[19] H. Geng, R. Rosen, B. Zheng, H. Shimoda, L. Fleming, J. Liu, O. Zhou, *Adv. Mater.* **2002**, *14*, 1387.
[20] F. H. Gojny, M. H. G. Wichmann, U. Köpke, B. Fiedler, K. Schulte, *Compos. Sci. Technol.* **2004**, *64*, 2363.
[21] E. T. Thostenson, T. W. Chou, *Carbon* **2006**, *44*, 3022.
[22] R. Haggenmueller, H. H. Gommans, A. G. Rinzler, J. E. Fischer, K. I. Winey, *Chem. Phys. Lett.* **2000**, *330*, 219.
[23] Z. Jin, K. P. Pramoda, G. Xu, S. H. Goh, *Chem. Phys. Lett.* **2001**, *337*, 43.
[24] P. Potschke, T. D. Fornes, D. R. Paul, *Polymer* **2002**, *43*, 3247.
[25] G. Mago, F. T. Fisher, D. M. Kalyon, *Macromolecules* **2008**, *41*, 8103.
[26] X. Chen, C. Burger, D. Fang, I. Sics, X. Wang, W. He, R. H. Somani, K. Yoon, B. S. Hsiao, B. Chu, *Macromolecules* **2006**, *39*, 5427.
[27] Z. Jia, Z. Wang, C. Xu, J. Liang, B. Wei, D. Wu, S. Zhu, Mater. *Sci. Engin. A* **1999**, *271*, 395.
[28] G. Z. Chen, M. S. P. Shaffer, D. Coleby, G. Dixon, W. Zhou, D. J. Fray, A. H. Windle, *Adv. Mater.* **2000**, *12*, 522.
[29] C. Velasco-Santos, A. L. Martinez-Hernandez, F. T. Fisher, R. Ruoff, V. M. Castano, *Chem. Mater.* **2003**, *15*, 4470.
[30] Q. Yao, L. Chen, W. Zhang, S. Liufu, X. Chen, *ACS Nano* **2010**, *4*, 2445.
[31] T. Kimura, H. Ago, M. Tobita, S. Ohshima, M. Kyotani, M. Yumura, *Adv. Mater.* **2002**, *14*, 1380.
[32] E. S. Choi, J. S. Brooks, D. L. Eaton, M. S. Al-Haik, M. Y. Hussaini, H. Garmestani, D. Li, K. Dahmen, *J. Appl. Phys.* **2003**, *94*, 6034.
[33] C. A. Martin, J. Sandler, A. H. Windle, M. Schwarz, W. Bauhofer, K. Schulte, M. S. P. Shaffer, *Polymer* **2005**, *46*, 877.
[34] A. Mamedov, N. Kotov, M. Prato, D. M. Guldi, J. P. Wicksted, A. Hirsch, *Nat. Mater.* **2002**, *1*, 190.
[35] M. Olek, J. Ostrander, S. Jurga, H. Möhwald, N. Kotov, K. Kempa, M. Giersig, *Nano Letters* **2004**, *4*, 1889.
[36] B. S. Shim, J. Zhu, E. Jan, K. Critchley, S. Ho, P. Podsiadlo, K. Sun, N. Kotov, *ACS Nano* **2009**, *3*, 1711.

[37] B. S. Shim, J. Zhu, E. Jan, K. Critchley, N. Kotov, *ACS Nano* **2010**, *4*, 3725.
[38] L. Wang, W. Chen, D. Xu, B. S. Shim, Y. Zhu, F. Sun, L. Liu, C. Peng, Z. Jin, C. Xu, N. Kotov, *Nano Letters* **2009**, *9*, 4147.
[39] E. Jan, J. L. Hendricks, V. Husaini, S. M. Richardson-Burns, A. Sereno, D. C. Martin, N. Kotov, *Nano Letters* **2009**, *9*, 4012.
[40] Z. Spitalsky, G. Tsoukleri, D. Tasis, C. Krontiras, S. Georga, C. Galiotis, *Nanotechnology* **2009**, *20*, 405702.
[41] J. N. Coleman, W. J. Blau, A. B. Dalton, E. Munoz, S. Collins, B. G. Kim, J. Razal, M. Selvidge, G. Vieiro, R. H. Baughman, *Appl. Phys. Lett.* **2003**, *82*, 1682.
[42] D. A. Walters, M. J. Casavant, X. C. Qin, C. B. Huffman, P. J. Boul, L. M. Ericson, E. H. Haroz, M. J. O'Connell, K. Smith, D. T. Colbert, R. E. Smalley, *Chem. Phys. Lett.* **2001**, *338*, 14.
[43] Z. Wang, Z. Liang, B. Wang, C. Zhang, L. Kramer, *Compos. Part A* **2004**, *35*, 1225.
[44] P. Gonnet, Z. Y. Liang, E. S. Choi, R. S. Kadambala, C. Zhang, J. S. Brooks, B. Wang, L. Kramer, *Curr. Appl. Phys.* **2006**, *6*, 119.
[45] Q. Cheng, J. Bao, J. Park, Z. Liang, C. Zhang, B. Wang, *Adv. Funct. Mater.* **2009**, *19*, 3219.
[46] Q. Cheng, B. Wang, C. Zhang, Z. Liang, *Small* **2010**, *6*, 763.
[47] D. Wang, P. Song, C. Liu, W. Wu, S. Fan, *Nanotechnology* **2008**, *19*, 075609.
[48] P. D. Bradford, X.Wang, H. Zhao, J.-P. Maria, Q. Jia, Y. T. Zhu, *Compos. Sci. Technol.* **2010**, *70*, 1980.
[49] K. Liu, Y. Sun, L. Chen, C. Feng, X. Feng, K. Jiang, Y. Zhao, S. Fan, *Nano Letters* **2008**, *8*, 700.
[50] Q. Cheng, J. Wang, K. Jiang, Q. Li, S. Fan, *J. Mater. Res.* **2008**, *23*, 2975.
[51] Q. Cheng, J. Wang, J. J. Wen, C. H. Liu, K. Jiang, S. Fan, *Carbon* **2010**, *48*, 260.
[52] N. R. Raravikar, L. S. Schadler, A. Vijayaraghavan, Y. Zhao, B. Wei, P. M. Ajayan, *Chem. Mater.* **2005**, *17*, 974.
[53] B. L. Wardle, D. S. Saito, E. J. Garcia, A. J. Hart, R. G. de Villoria, E. A. Verploegen, *Adv. Mater.* **2008**, *20*, 2707.
[54] E. Lahiff, C. Y. Ryu, S. Curran, A. I. Minett, W. J. Blau, P. M. Ajayan, *Nano Letters* **2003**, *3*, 1333.
[55] X. Gui, A. Cao, J. Wei, H. Li, Y. Jia, Z. Li, L. Fan, K. Wang, H. Zhu, D. Wu, *ACS Nano* **2010**, *4*, 2320.
[56] L. Valentini, S. B. Bon, J. M. Kenny, *Carbon* **2007**, *45*, 2685.
[57] B. Vigolo, A. Penicaud, C. Coulon, C. Sauder, R. Pailler, C. Journet, P. Bernier, P. Poulin, *Science* **2000**, *290*, 1331.
[58] B. Vigolo, P. Poulin, M. Lucas, P. Launois, P. Bernier, *Appl. Phys. Lett.* **2002**, *81*, 1210.
[59] J. N. Barisci, M. Tahhan, G. G. Wallace, S. Badaire, T. Vaugien, M. Maugey, P. Poulin, *Adv. Funct. Mater.* **2004**, *14*, 133.
[60] A. B. Dalton, S. Collins, E. Munoz, J. Razal, V. Ebron, J. Ferraris, J. N. Coleman, B. G. Kim, R. H. Baughman, *Nature* **2003**, *423*, 703.

[61] P. Miaudet, S. Badaire, M. Maugey, A. Derre, V. Pichot, P. Launois, P. Poulin, C. Zakri, *Nano Letters* **2005**, *5*, 2212.
[62] X. Zhang, T. Liu, T. V. Sreekumar, S. Kumar, X. Hu, K. Smith, *Polymer* **2004**, *45*, 8801.
[63] Y. Wang, R. Cheng, L. Liang, Y. Wang, *Compos. Sci. Technol.* **2005**, *65*, 793.
[64] S. Kumar, T. D. Dang, F. E. Arnold, A. R. Bhattacharyya, B. G. Min, X. Zhang, R. A. Vaia, C. Park, W. Wade Adams, R. H. Hauge, R. E. Smalley, S. Ramesh, P. A. Willis, *Macromolecules* **2002**, *35*, 9039.
[65] M. C. Weisenberger, E. A. Grulke, D. Jacques, T. Rantell, R. Andrews, *J. Nanosci. Nanotechnol.* **2003**, *3*, 535.
[66] T. V. Sreekumar, T. Liu, B. G. Min, H. Guo, S. Kumar, R. H. Hauge, R. E. Smalley, *Adv. Mater.* **2004**, *16*, 58.
[67] F. Ko, Y. Gogotsi, A. Ali, N. Naguib, H. Ye, G. L. Yang, C. Li, P. Willis, *Adv. Mater.* **2003**, *15*, 1161.
[68] Y. Dror, W. Salalha, R. L. Khalfin, Y. Cohen, A. L. Yarin, E. Zussman, *Langmuir* **2003**, *19*, 7012.
[69] Y.-L. Li, L. A. Kinloch, A. H. Windle, *Science* **2004**, *304*, 276.
[70] K. Koziol, J. Vilatela, A. Moisala, M. Motta, P. Cunniff, M. Sennett, A. H. Windle, *Science* **2007**, *318*, 1892.
[71] R. J. Mora, J. J. Vilatela, A. H. Windle, *Compos. Sci. Technol.* **2009**, *69*, 1558.
[72] W. Ma, L. Song, R. Yang, T. Zhang, Y. Zhao, L. Sun, Y. Ren, D. Liu, L. Liu, J. Shen, Z. Zhang, Y. Xiang, W. Zhou, S. Xie, *Nano Letters* **2007**, *7*, 2307.
[73] W. Ma, L. Q. Liu, Z. Zhang, R. Yang, G. Liu, T. H. Zhang, X. An, X. Yi, Y. Ren, Z. Niu, J. Li, H. Dong, W. Zhou, P. M. Ajayan, S. Xie, *Nano Letters* **2009**, *9*, 2855.